IEEE Access
Multidisciplinary | Rapid Review | Open Access Journal

Received October 15, 2020, accepted November 4, 2020, date of publication November 16, 2020,
date of current version November 24, 2020.

Digital Object Identifier 10.1109/ACCESS.2020.3037814

Traffic Aware Beamformer Design for Flexible TDD-Based Integrated Access and Backhaul

PRANEETH JAYASINGHE[1], (Member, IEEE), ANTTI TÖLLI[1], (Senior Member, IEEE), JARKKO KALEVA[2], (Member, IEEE), AND MATTI LATVA-AHO[1], (Senior Member, IEEE)
[1]Center for Wireless Communications, University of Oulu, 90570 Oulu, Finland
[2]Solmu Technologies Oy, 90620 Oulu, Finland

Corresponding author: Praneeth Jayasinghe (praneeth.laddu@oulu.fi)

This work was supported in part by the European Commission in the framework of the H2020-EUJ-02-2018 Project under Grant 815056 (5G-Enhance), and in part by the Academy of Finland under Grant 318927 (6Genesis Flagship).

ABSTRACT Integrated access and backhaul (IAB) network consists of base station (BS), relay nodes (RNs), and user-equipments (UEs), where BS and RNs exchange UE data via wireless in-band backhaul while sharing the same frequency-time resources with access links. In this paper, a flexible time-division-duplex (TDD)-based IAB network is considered where RNs and BS are assigned to distinct uplink (UL) or downlink (DL) transmission modes to mitigate conventional half-duplex (HD) loss at RNs. An iterative beamformer design is proposed to manage the resulting cross-channel interference and to allocate wireless backhaul and access resources jointly over two consecutive data delivery intervals required for communications between the BS and UEs through HD RNs. Dynamic traffic behavior is handled via weighted queue minimization objective, and user-specific UL/DL queues are also introduced at RNs to guarantee reliable end-to-end data delivery. Bi-directional forward-backward training via spatially precoded over-the-air pilot signaling is employed to allow decentralized beamformer design across all the nodes. A novel user allocation method is proposed to assign UEs to BS or RNs based only on long-term channel statistics and some practical IAB limitations. The numerical examples illustrate the superior system performance of the considered flexible IAB in comparison to the conventional HD relaying system.

INDEX TERMS Coordinated beamforming, flexible and dynamic TDD, integrated access and backhaul, weighted queue minimization.

I. INTRODUCTION

Small cell deployment has been recognized as a key research direction to fulfill ever-growing traffic demand in the next-generation cellular systems [1]–[3]. However, connecting these small-cell base stations (BS) to the core network using optical fiber can be onerous and costly [4]. Current developments of millimeter-wave (mm-Wave) communication have enabled the possibility to use high-speed wireless backhaul for densified small-cell networks, which can be more cost-effective, flexible, and easier to be deployed [5]. We refer to these networks as integrated access and backhaul (IAB) systems or self-backhaul systems.

Self-backhauling or IAB network consists of three components, which have been coined as IAB-donor (referred to as BS), IAB-nodes (i.e., relay nodes (RNs)), and user-equipments (UEs) in the third-generation partnership project (3GPP) [6], [7]. Relay nodes assist the BS to provide wireless access to UEs while the BS offers both direct access for UEs to the core network and wireless backhauling functionality to RNs. Moreover, IAB offers the flexibility to use the same wireless resources for access and backhaul data transmissions simultaneously in both uplink (UL) and downlink (DL) directions based on the traffic requirements. Therefore, IAB plays a vital role in wireless communication networks to expand coverage and improve the throughput with lower transmit power requirements and with minimal planning and implementation cost. Consequently, IAB systems have received significant attention in the 3GPP new radio (NR) specifications [6], [7].

IAB network can be also referred to as a cooperative relaying network with some advanced capabilities. Notably, various research studies have shown that cooperative relaying systems can improve reliability, throughput, and

The associate editor coordinating the review of this manuscript and approving it for publication was Nan Wu.

communication coverage with lower power requirements [8]–[10]. Higher layer (layer 2 or layer 3) relaying protocol such as decode-and-forward (DF) protocol is more suited for the IAB network as the relay node (RN) must be capable of simultaneously handling multiple UL and DL UEs. Furthermore, it is essential to have user-specific queues for both UL and DL UEs at RNs to guarantee end-to-end data delivery. Full-duplex (FD) relaying with DF protocol at the RN has been considered in some recent studies on IAB functionality [11]–[13]. Even though FD relaying facilitates both backhaul and access data transmission simultaneously, the practical implementation is still challenging due to excessive complexity and production cost [14], [15]. Moreover, two-way half-duplexed (HD) relaying protocol has emerged as a potential alternative to FD relaying protocol, which utilizes the spectrum more efficiently and considerably reduces the conventional HD loss [16]–[18]. In the two-way HD relaying protocol, both BS and UEs (served by RN) transmit backhaul and access data to the RN in the first timeslot (multiple access stage) while in the next timeslot, the RN broadcasts received messages to BS and UEs (broadcasting stage), thus both UL and DL UE data are served within two consecutive time intervals. As the current 3GPP NR study encourages application-specific flexible frame structures, by employing flexible time-division-duplexing (TDD) based resource scheduling, IAB networks can support two-way HD relaying [19]. Nevertheless, it is challenging to handle complicated cross-link interference scenarios introduced in the IAB system. Multiple-input-multiple-output (MIMO) systems provide more spatial degrees of freedom to mitigate interference in complex interference-limited systems [20], [21]. Hence, the interference in IAB networks can be efficiently mitigated by employing multiple antennas at each node.

It is essential to collect required channel state information (CSI), either centralized or decentralized, to design beamformers for a multi-user MIMO system. In a flexible TDD-based IAB, the channel reciprocity can be used to acquire the CSI between each node via reverse link pilot measurements. A specific challenge with the considered flexible-TDD (where both UL and DL transmissions co-exist) arrangement is the CSI acquisition of the cross-link interference channels, e.g., among mutually interfering user terminals. Explicit feedback of the UE-to-UE and RN-to-UE channels to the BS would be required to enable optimal beamformer design, which would make the centralized implementation infeasible in practice. However, the decentralized coordinated beamformer design can be made possible by employing bi-directional forward-backward (F-B) training via spatially precoded over-the-air (OTA) pilot signaling [22]–[24]. In practice, the number of orthogonal pilot sequences is limited as their availability for CSI estimation depends on the coherence time and coherence bandwidth of the wireless channel [25]. Smart pilot reuse schemes or robust estimation techniques with non-orthogonal pilots can be employed to carry out the beamformer design by adequately mitigating the pilot contamination effect [26].

A. PRIOR WORK

The recent advances of self-interference (SI) cancellation techniques have motivated to carry out research on FD in-band communication [27], [28], also applied to self-backhauling networks [11]–[13], [29]. For example, in [11], downlink spectrum allocation schemes were studied for FD small cell networks in both centralized and decentralized manner by considering in-band FD, out-band FD, and hybrid schemes. In [12], [13], robust beamformer designs were proposed for an FD MIMO relaying system assuming imperfect CSI estimation. Authors in [13], [29], investigated the resource allocation/optimization with mm-Wave and massive MIMO techniques. As an alternative to FD systems, there are numerous studies on two-way HD relaying in [16]–[18], [20], [30]–[33], which have shown that two-way HD relaying improves the spectral efficiency significantly compared to the conventional HD system.

There have been numerous studies on multi-user MIMO based beamformer designs for optimizing network utilities such as weighted sum rate (WSR), weighted minimum mean square error (WMMSE), and weighted queue minimization (WQM) in both centralized and decentralized manner with different coordination assumptions [22], [34]–[36]. Furthermore, practical implementation of the coordinated precoding and CSI acquisition by employing bi-directional OTA signaling has been studied in, e.g., [22], [23], [26]. Different techniques were investigated in [23], [37]–[40] to mitigate the pilot contamination effect at the CSI estimation process. In particular, a practical approach based on direct least squares (LS) beamformer estimation from the contaminated UL/DL pilots was investigated in [23]. In our earlier work [21], we proposed a decentralized iterative beamformer design to handle UL-DL and DL-UL cross-link interference in the dynamic TDD system. By carefully following the fifth-generation (5G) NR frame structure [19], bi-directional F-B training was employed to exchange intermediate beamformers between BSs and UEs, while the direct beamformer estimation (DE) method was used to mitigate the pilot contamination.

B. CONTRIBUTIONS

We consider a flexible TDD-based IAB network, such that in a given timeslot, BS and RNs operate in distinct UL/DL modes. For example, when BS is in the DL mode, RNs are in the UL mode and vice-versa, as illustrated in Fig. 1. Thereby, RNs are continuously in the two-way HD relaying mode, which significantly alleviates the HD loss in such relaying setup. An iterative beamformer design with the WQM objective and resource allocation design are proposed to manage the resulting cross-channel interference and to allocate wireless backhaul and access resources jointly over two consecutive data delivery intervals required for communications between the BS and UEs through HD RNs. From the queue minimization point of view, it is important to consider end-to-end data transmission. To this end, we introduce user-specific UL/DL queues to RNs, in addition to queues

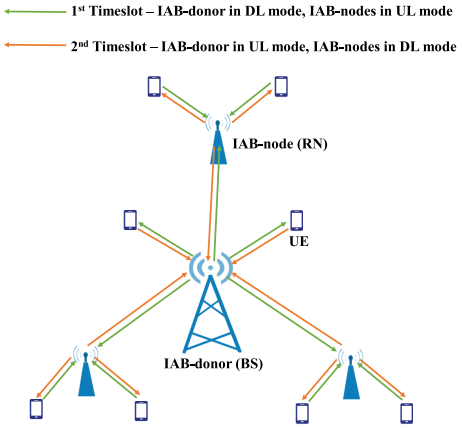

FIGURE 1. Flexible TDD-based IAB Network with two-way HD relaying.

at UEs and BS, and incorporate them into the end-to-end WQM objective. Similarly to DL only scenarios considered in [36], [41], the WQM problem in the considered IAB setup is solved via iterative evaluation of KKT conditions leading to a low complexity distributed algorithm with minimal queue state-related scalar information exchange between network nodes. Furthermore, the iterative design incorporates a water-filling type scheme to multiplex user-specific data streams over the backhaul in both DL and UL directions. To facilitate practical implementation, we provide an over-the-air (OTA) signaling scheme as in [22]–[24], wherein precoded pilots are used to iteratively exchange the intermediate beamformers in both backward and forward direction. Then, direct beamformer estimation methods are applied to alleviate the pilot contamination effect, as in our previous work [21]. In this paper, we further propose a novel centralized approach to assign users into respective BS or RN by using path gain information and concerning potential practical constraints that are unique to IAB systems, such as limited spatial degrees of freedom in the BS-RN channel due to the line-of-sight (LOS) deployment and significant UL-to-DL interference of the nearby UE pairs. The user assignment is attained by solving a combinatorial optimization problem, which is in an integer linear programming (ILP) form. Since the complexity of ILP increases exponentially, we propose two approximate approaches to solve it efficiently: 1) Direct linear program (LP) solution; and 2) SCA based LP solution [42].

Major contributions of this paper are summarized as follows:

- An iterative beamformer design is proposed for the flexible TDD-based IAB system by assuming two consecutive data delivery intervals and user-specific queues at each node with the end-to-end WQM objective.
- The end-to-end WQM problem is solved via iterative evaluation of KKT conditions and a water-filling type scheme is proposed to multiplex user-specific data over wireless backhaul links.
- OTA bi-directional signaling architecture and direct beamformer estimation techniques are proposed to provide a practical decentralized beamformer design implementation and to mitigate the pilot contamination effect.
- A centralized user assignment algorithm is proposed for the considered IAB setting by using the long term channel statistics, nearby user information, and rank of the BS-RN channel.
- A thorough numerical study is carried out where the proposed flexible TDD-based IAB network is shown to significantly outperform the half duplex relaying reference case.

C. ORGANIZATION AND NOTATION

The rest of the paper is organized as follows. Section II presents the system model used in the rest of the paper. In Section III, the proposed precoder design with the end-to-end WQM objective is presented for IAB, along with the novel BS-RN user assignment method. In Section IV, training and signaling architecture for decentralized beamformer design is introduced and complexity analysis is provided. Finally, Section V presents the numerical examples, while Section VI concludes the paper.

Notations: $\mathbb{C}^{m\times n}$ denotes an $m \times n$ matrix with elements in the complex field. Capital bold letters represent matrices, simple bold letters represent vectors and simple letters represent scalar variables. $(\cdot)^{-1}$, $(\cdot)^{\mathrm{T}}$, and $(\cdot)^{\mathrm{H}}$ indicate inverse, transpose, and Hermitian of a matrix respectively. $\mathbb{E}\{.\}$ is the expectation of a random variable. Cardinality of a discrete set $\mathcal{A}$ is denoted as $|\mathcal{A}|$. $\mathcal{CN}(x, y)$ denotes a complex Gaussian random variable with mean x and variance y. A similar notation is valid when the variable is a vector or matrix.

II. SYSTEM MODEL

We consider a flexible TDD based multi-user MIMO IAB system consisting of one BS and multiple DF RNs as shown in Fig. 1. The set of UEs served by the BS or RN i is denoted by $\mathcal{U}_i$. Here, for the simplicity of the notation, we use $i = 1$ for the BS and $i \in \{2, 3, \ldots, N\} = \mathcal{B}_{\mathrm{R}}$ for RNs. The total number of UEs in the system is K and, the number of UEs served by the BS or RN i is $K_i = |\mathcal{U}_i|$. Also, the serving BS/RN of the user k is denoted as i_k. Each UE k employs N_k antenna elements while each BS/RN i employs M_i antenna elements. The maximum number of spatial data streams allocated to UE $k \in \mathcal{U}_i$ is denoted by $L_k \leq \min(M_i, N_k)$. Also, the maximum number of spatial data streams between the BS and RN i is denoted as $\bar{L}_i \leq \min(M_i, M_1)$.

In the IAB system, we consider two-way HD relaying at RNs to eliminate the half-duplex loss effectively. Hence, in a given timeslot, BS and RNs operate in distinct UL/DL modes. Note that for UEs served by RN, data transmission from/to BS to/from UEs takes two timeslots. Therefore, we consider two timeslots to model the end-to-end system behavior. In the first time slot, the BS is in DL mode while RNs are in UL mode (multiple access stage). In the second time slot, the BS is in UL mode, and RNs are in DL mode (broadcasting

stage). Therefore, the following transmissions and transmit precoders are applied during the first timeslot;

- Tx1: The BS transmits data to DL UEs. Transmit precoder for DL UE $k \in \mathcal{U}_1$ via l^{th} spatial stream is $\mathbf{m}_{k,l}^{(\mathrm{dl},1)} \in \mathbb{C}^{M_1}$.
- Tx2: UL UEs transmits data to the serving RN. Transmit precoder from UL UE $k \in \mathcal{U}_i$ via l^{th} spatial stream is $\mathbf{m}_{k,l}^{(\mathrm{ul},1)} \in \mathbb{C}^{N_k}$.
- Tx3: The BS wirelessly backhaul data to each RN to serve their DL UEs in the next timeslot. Transmit precoder for RN i at BS, via l^{th} spatial stream is $\mathbf{v}_{i,l}^{(\mathrm{dl})} \in \mathbb{C}^{M_1}$.

Due to the above transmissions in the first timeslot, the received signal $\mathbf{x}_k^{(\mathrm{dl},1)} \in \mathbb{C}^{N_k}$ at DL UE $k \in \mathcal{U}_1$ can be expressed as

$$\mathbf{x}_k^{(\mathrm{dl},1)} = \mathbf{H}_{1,k}\Big(\sum_{j\in\mathcal{U}_1}\sum_{n=1}^{L_j}\mathbf{m}_{j,n}^{(\mathrm{dl},1)}d_{j,n}^{(\mathrm{dl},1)} + \sum_{i=2}^{N}\sum_{n=1}^{\bar{L}_i}\mathbf{v}_{i,n}^{(\mathrm{dl})}d_{i,n}^{(\mathrm{dl})}\Big) + \sum_{i=2}^{N}\sum_{j\in\mathcal{U}_i}\sum_{n=1}^{L_j}\tilde{\mathbf{H}}_{j,k}\mathbf{m}_{j,n}^{(\mathrm{ul},1)}d_{j,n}^{(\mathrm{ul},1)} + \mathbf{z}_k, \quad (1)$$

where $\mathbf{H}_{i,k} \in \mathbb{C}^{N_k\times M_i}$ is the channel matrix between BS/RN i and UE k, $\tilde{\mathbf{H}}_{j,k} \in \mathbb{C}^{N_k\times N_j}$ is the UE-UE interference channel matrix between UE j and UE k. All transmit data symbols $d_{j,n}^{(\mathrm{dl},1)}$, $d_{j,n}^{(\mathrm{ul},1)}$ and $d_{i,n}^{(\mathrm{dl})}$ ($\forall j, n, i$) are assumed to be independent and identically distributed (i.i.d.) with $\mathbb{E}\{|d_{j,n}^{(\mathrm{dl},1)}|^2\} = 1$, $\mathbb{E}\{|d_{j,n}^{(\mathrm{ul},1)}|^2\} = 1$ and $\mathbb{E}\{|d_{i,n}^{(\mathrm{dl})}|^2\} = 1$. We assume complex white Gaussian noise $\mathbf{z}_k \in \mathbb{C}^{N_k}$ with variance $\mathcal{N}_0$ per element. Similarly, the received signal $\mathbf{x}_i^{(\mathrm{ul},1)} \in \mathbb{C}^{M_i}$ at RN i can be expressed as

$$\mathbf{x}_i^{(\mathrm{ul},1)} = \hat{\mathbf{H}}_{1,i}\Big(\sum_{j\in\mathcal{U}_1}\sum_{n=1}^{L_j}\mathbf{m}_{j,n}^{(\mathrm{dl},1)}d_{j,n}^{(\mathrm{dl},1)} + \sum_{r=2}^{N}\sum_{n=1}^{\bar{L}_r}\mathbf{v}_{r,n}^{(\mathrm{dl})}d_{r,n}^{(\mathrm{dl})}\Big) + \sum_{r=2}^{N}\sum_{j\in\mathcal{U}_r}\sum_{n=1}^{L_j}\mathbf{H}_{i,j}^{\mathrm{H}}\mathbf{m}_{j,n}^{(\mathrm{ul},1)}d_{j,n}^{(\mathrm{ul},1)} + \mathbf{z}_i, \quad (2)$$

where $\hat{\mathbf{H}}_{1,i} \in \mathbb{C}^{M_i\times M_1}$ is the channel matrix between the BS and RN i. To decode the received data, the following linear receivers are employed at the receiver nodes;

- Rx1: The DL UE $k \in \mathcal{U}_1$ employs linear receiver $\mathbf{u}_{k,l}^{(\mathrm{dl},1)} \in \mathbb{C}^{N_k}$. Then the estimated data for l^{th} spatial stream is $\hat{d}_{k,l}^{(\mathrm{dl},1)} = (\mathbf{u}_{k,l}^{(\mathrm{dl},1)})^{\mathrm{H}}\mathbf{x}_k^{(\mathrm{dl},1)}$.
- Rx2: The i^{th} RN employs linear receiver $\mathbf{u}_{k,l}^{(\mathrm{ul},1)} \in \mathbb{C}^{M_i}$ to decode the data from UL UE $k \in \mathcal{U}_i$ via l^{th} spatial stream. Then the estimated data is $\hat{d}_{k,l}^{(\mathrm{ul},1)} = (\mathbf{u}_{k,l}^{(\mathrm{ul},1)})^{\mathrm{H}}\mathbf{x}_i^{(\mathrm{ul},1)}$.
- Rx3: The RN i employs $\mathbf{w}_{i,l}^{(\mathrm{dl})} \in \mathbb{C}^{M_i}$ to decode backhaul data from BS via l^{th} spatial stream. Then the estimated data is $\hat{d}_{i,l}^{(\mathrm{dl})} = (\mathbf{w}_{i,l}^{(\mathrm{dl})})^{\mathrm{H}}\mathbf{x}_i^{(\mathrm{ul},1)}$.

Similarly, the following transmissions and transmit precoders are used in the second timeslot;

- Tx4: UL UEs transmit data to BS. Transmit precoder of UL UE $k \in \mathcal{U}_1$ in l^{th} spatial stream is $\mathbf{m}_{k,l}^{(\mathrm{ul},2)} \in \mathbb{C}^{N_k}$.
- Tx5: Each RN transmit data to DL UEs. Transmit precoder for DL UE $k \in \mathcal{U}_i$ via l^{th} spatial stream is $\mathbf{m}_{k,l}^{(\mathrm{dl},2)} \in \mathbb{C}^{M_i}$.
- Tx6: Relaying the received UL UE data to the BS by each RN. Transmit precoder of the RN i to BS, via l^{th} spatial stream is $\mathbf{v}_{i,l}^{(\mathrm{ul})} \in \mathbb{C}^{M_i}$.

Then, the received signal $\mathbf{x}_1^{(\mathrm{ul},2)} \in \mathbb{C}^{M_1}$ at the BS can be expressed as

$$\mathbf{x}_1^{(\mathrm{ul},2)} = \sum_{i=2}^{N}\hat{\mathbf{H}}_{1,i}^{\mathrm{T}}\Big(\sum_{n=1}^{\bar{L}_i}\mathbf{v}_{i,n}^{(\mathrm{ul})}d_{i,n}^{(\mathrm{ul})} + \sum_{j\in\mathcal{U}_i}\sum_{n=1}^{L_j}\mathbf{m}_{j,n}^{(\mathrm{dl},2)}d_{j,n}^{(\mathrm{dl},2)}\Big) + \sum_{j\in\mathcal{U}_1}\sum_{n=1}^{L_j}\mathbf{H}_{1,j}^{\mathrm{H}}\mathbf{m}_{j,n}^{(\mathrm{ul},2)}d_{j,n}^{(\mathrm{ul},2)} + \mathbf{z}_1, \quad (3)$$

where $d_{j,n}^{(\mathrm{dl},2)}$, $d_{j,n}^{(\mathrm{ul},2)}$ and $d_{i,n}^{(\mathrm{ul})}$ ($\forall j, n, i$) are the transmit data symbols, which are i.i.d. with $\mathbb{E}\{|d_{j,n}^{(\mathrm{dl},2)}|^2\} = 1$, $\mathbb{E}\{|d_{j,n}^{(\mathrm{ul},2)}|^2\} = 1$ and $\mathbb{E}\{|d_{i,n}^{(\mathrm{ul})}|^2\} = 1$.

Similarly, the received signal $\mathbf{x}_k^{(\mathrm{dl},2)} \in \mathbb{C}^{N_k}$ at DL UE $k \in \mathcal{U}_i$ can be expressed as,

$$\mathbf{x}_k^{(\mathrm{dl},2)} = \sum_{r=2}^{N}\mathbf{H}_{r,k}\Big(\sum_{n=1}^{\bar{L}_i}\mathbf{v}_{i,n}^{(\mathrm{ul})}d_{i,n}^{(\mathrm{ul})} + \sum_{j\in\mathcal{U}_r}\sum_{n=1}^{L_j}\mathbf{m}_{j,n}^{(\mathrm{dl},2)}d_{j,n}^{(\mathrm{dl},2)}\Big) + \sum_{j\in\mathcal{U}_1}\sum_{n=1}^{L_j}\tilde{\mathbf{H}}_{j,k}^{\mathrm{T}}\mathbf{m}_{j,n}^{(\mathrm{ul},2)}d_{j,n}^{(\mathrm{dl},2)} + \mathbf{z}_k. \quad (4)$$

To decode each of the received data, we employ following linear receivers at the receiver node.

- Rx4: The BS employs $\mathbf{u}_{k,l}^{(\mathrm{ul},2)} \in \mathbb{C}^{M_1}$ to decode data from l^{th} spatial stream of UL UE $k \in \mathcal{U}_1$. Then the estimated data is $\hat{d}_{k,l}^{(\mathrm{ul},2)} = (\mathbf{u}_{k,l}^{(\mathrm{ul},2)})^{\mathrm{H}}\mathbf{x}_1^{(\mathrm{ul},2)}$.
- Rx5: The DL UE $k \in \mathcal{U}_i$ employs $\mathbf{u}_{k,l}^{(\mathrm{dl},2)} \in \mathbb{C}^{N_k}$ to decode the received data via spatial stream l. Then the estimated data is $\hat{d}_{k,l}^{(\mathrm{dl},2)} = (\mathbf{u}_{k,l}^{(\mathrm{dl},2)})^{\mathrm{H}}\mathbf{x}_k^{(\mathrm{dl},2)}$.
- Rx6: The BS employs $\mathbf{w}_{i,l}^{(\mathrm{ul})} \in \mathbb{C}^{M_1}$ to decode the relaying data from RN i via l^{th} spatial stream. Then the estimated data is $\hat{d}_{i,l}^{(\mathrm{ul})} = (\mathbf{w}_{i,l}^{(\mathrm{ul})})^{\mathrm{H}}\mathbf{x}_1^{(\mathrm{ul},2)}$.

Here, the corresponding user-specific MSE for UL/DL data detection is denoted in a common form as $\epsilon_{k,l}^{(a,s)} = \mathbb{E}[|\hat{d}_{k,l}^{(a,s)} - \hat{d}_{k,l}^{(a,s)}|^2]$ with $a = \{\mathrm{ul}, \mathrm{dl}\}$ and $s = \{1, 2\}$. Also, MSE for the data detection corresponding to backhaul traffic is denoted as $\epsilon_{i,l}^{(a)} = \mathbb{E}[|\hat{d}_{i,l}^{(a)} - \hat{d}_{i,l}^{(a)}|^2]$. Hence, the user-specific MSE value corresponding to Rx1 can be obtained as

$$\epsilon_{k,l}^{(\mathrm{dl},1)} = 1 - 2\Re((\mathbf{u}_{k,l}^{(\mathrm{dl},1)})^{\mathrm{H}}\mathbf{H}_{1,k}\mathbf{m}_{k,l}^{(\mathrm{dl},1)}) + (\mathbf{u}_{k,l}^{(\mathrm{dl},1)})^{\mathrm{H}}\mathbf{M}_k^{(\mathrm{dl},1)}\mathbf{u}_{k,l}^{(\mathrm{dl},1)}, \quad (5)$$

where $\mathbf{M}_k^{(\mathrm{dl},1)} = \mathbb{E}[\mathbf{x}_k^{(\mathrm{dl},1)}(\mathbf{x}_k^{(\mathrm{dl},1)})^{\mathrm{H}}]$ is the received signal covariance matrices for DL UE k. Expression for $\mathbf{M}_k^{(\mathrm{dl},1)}$ is

given in (6) on bottom of the page. Then, the MMSE receiver corresponding to Rx1 is given by

$$\tilde{\mathbf{u}}_{k,l}^{(\mathrm{dl},1)} = (\mathbf{M}_k^{(\mathrm{dl},1)})^{-1}\mathbf{H}_{1,k}\mathbf{m}_{k,l}^{(\mathrm{dl},1)}. \tag{7}$$

The reader is referred to Appendix A for the MSE, received signal covariance and MMSE receiver expressions corresponding to the receiver types from Rx2 to Rx6.

III. PRECODER DESIGN

In this section, we present an iterative transmit/receive beamformer design with the WQM objective for the considered flexible TDD based IAB system. For UEs served by the RNs, it minimally takes two timeslots for the end-to-end data delivery. Hence, in the WQM objective, we jointly consider queue states at each node during both timeslots. For a successful IAB communication, the following UL/DL queues are required at each node;

- At the BS, DL UE queues ($Q_k^{(\mathrm{dl})}$) are required for, both, directly serving and relaying UEs as all DL traffic passes through the BS.
- At each UE, UL queues ($Q_k^{(\mathrm{ul})}$) are maintained to send UL traffic to the serving BS/RN.
- At the RNs, user-specific UL ($\bar{Q}_k^{(\mathrm{ul})}$) and DL ($\bar{Q}_k^{(\mathrm{dl})}$) queues are employed to store/relay access and backhaul data, hence to guarantee end-to-end data delivery.

Note that the DL UE queues at RN are filled up as backhaul traffic arrives from the BS during the first timeslot, and emptied when serving DL UEs during the second timeslot. Similarly, the UL UE queues at RN grow due to the received UL UE data during the first timeslot, and drain when relaying the data to the BS during the second timeslot. Hence, from the overall queue minimization perspective, it is crucial to consider the traffic dynamic at each node over two timeslots. Then, we can define a queue deviation metric $\Psi_k^{(\mathrm{dl})}$ for all DL UE queues at the BS, after two timeslots, as

$$\Psi_k^{(\mathrm{dl})} = \begin{cases} Q_k^{(\mathrm{dl})} - \sum_{l=1}^{L_k} R_{k,l}^{(\mathrm{dl},1)} & k \in \mathcal{U}_1, \\ Q_k^{(\mathrm{dl})} - \sum_{l=1}^{L_i} a_k^{(\mathrm{dl})} R_{i,l}^{(\mathrm{dl})} & k \in \mathcal{U}_i,\, i \in \mathcal{B}_{\mathrm{R}}, \end{cases} \tag{8}$$

where $R_{k,l}^{(a,s)}$ denotes the number of transmitted bits over the l^{th} spatial stream to/from UE k. The backhaul rate over the l^{th} spatial stream to/from BS to RN i is denoted as $R_{i,l}^{(a)}$. Moreover, by assuming MMSE receivers are employed at each receiver node, instantaneous rate can be expressed as $R_{k,l}^{(a,s)} = -\log_2(\epsilon_{k,l}^{(a,s)})$ and $R_{i,l}^{(a)} = -\log_2(\epsilon_{i,l}^{(a)})$ [22]. Here, the backhaul streams are multiplexed with data from several UEs and, $a_k^{(a)}$ is the multiplexed rate portion for each UE k ($0 \le a_k^{(a)} \le 1$). Moreover, at each UL UE, queue deviation metric $\Psi_k^{(\mathrm{ul})}$ for the UL queues, after two timeslots, is given by

$$\Psi_k^{(\mathrm{ul})} = \begin{cases} Q_k^{(\mathrm{ul})} - \sum_{l=1}^{L_k} R_{k,l}^{(\mathrm{ul},2)} & k \in \mathcal{U}_1, \\ Q_k^{(\mathrm{ul})} - \sum_{l=1}^{L_k} R_{k,l}^{(\mathrm{ul},1)} & k \in \mathcal{U}_i,\, i \in \mathcal{B}_{\mathrm{R}}. \end{cases} \tag{9}$$

Similarly, queue deviation metric $\bar{\Psi}_k^{(\mathrm{dl})}$ and $\bar{\Psi}_k^{(\mathrm{ul})}$ for DL and UL UE queues at the RN i_k, after two timeslots are given by

$$\bar{\Psi}_k^{(\mathrm{dl})} = \bar{Q}_k^{(\mathrm{dl})} + \sum_{l=1}^{L_i} a_k^{(\mathrm{dl})} R_{i,l}^{(\mathrm{dl})} - \sum_{l=1}^{L_k} R_{k,l}^{(\mathrm{dl},2)}, \tag{10a}$$

$$\bar{\Psi}_k^{(\mathrm{ul})} = \bar{Q}_k^{(\mathrm{ul})} + \sum_{l=1}^{L_k} R_{k,l}^{(\mathrm{ul},1)} - \sum_{l=1}^{L_i} a_k^{(\mathrm{ul})} R_{i,l}^{(\mathrm{ul})}. \tag{10b}$$

In order to simplify the notation, let $\tilde{\Psi}^{(a)}$ and $\tilde{\bar{\Psi}}^{(a)}$ denote vectors with elements $\tilde{\Psi}_k^{(a)} \triangleq \alpha_k^{1/q}\Psi_k^{(a)}$ and $\tilde{\bar{\Psi}}_k^{(a)} \triangleq \alpha_k^{1/q}\bar{\Psi}_k^{(a)}$, respectively. Here, α_k is a weighting factor, reflecting user specific priorities.

Note that, before the precoder/decoder design, we assume UEs are already assigned to a particular BS or RN by using the user assignment algorithm, which is explained in detail in Section III.C. Here, we define weighted ℓ_q-norm queue minimization of the UL and DL users during two timeslots with sum transmit power constraints at the transmitters as

$$\min_{\mathcal{M},\mathcal{W}} \sum_{a\in\{\mathrm{ul},\mathrm{dl}\}} \|\tilde{\Psi}^{(a)}\|_q + \|\tilde{\bar{\Psi}}^{(a)}\|_q \tag{11a}$$

$$\text{s. t.} \quad \sum_{l=1}^{L_k} \|\mathbf{m}_{k,l}^{(\mathrm{ul},1)}\|^2 \le P_k^{(\mathrm{ul})} \qquad \forall k \in \mathcal{U}_i,\, i \ne 1, \tag{11b}$$

$$\sum_{k\in\mathcal{U}_1}\sum_{l=1}^{L_k} \|\mathbf{m}_{k,l}^{(\mathrm{dl},1)}\|^2 + \sum_{i=2}^{N}\sum_{l=1}^{\bar{L}_i} \|\mathbf{v}_{i,l}^{(\mathrm{dl})}\|^2 \le P_1^{(\mathrm{dl})}, \tag{11c}$$

$$\sum_{l=1}^{L_k} \|\mathbf{m}_{k,l}^{(\mathrm{ul},2)}\|^2 \le P_k^{(\mathrm{ul})} \qquad \forall k \in \mathcal{U}_1, \tag{11d}$$

$$\sum_{k\in\mathcal{U}_i}\sum_{l=1}^{L_k} \|\mathbf{m}_{k,l}^{(\mathrm{dl},2)}\|^2 + \sum_{l=1}^{\bar{L}_i} \|\mathbf{v}_{i,l}^{(\mathrm{ul})}\|^2 \le P_i^{(\mathrm{dl})} \quad \forall i \in \mathbb{B}_{\mathrm{R}}, \tag{11e}$$

where $\mathcal{M}$ represent the set of all transmit precoders and $\mathcal{W}$ represent the set of all receive beamformers. Maximum transmit power at BS/RN i is denoted as $P_i^{(\mathrm{dl})}$ and maximum transmit power at UE k denoted as $P_k^{(\mathrm{ul})}$.

The WQM problem in (11) is proposed to design precoders to minimize the total number of backlogged packets in the IAB network over two consecutive timeslots by optimizing transmit and receive beamformers at each node.

$$\mathbf{M}_k^{(\mathrm{dl},1)} = \mathbf{H}_{1,k}\Big(\sum_{j\in\mathcal{U}_1}\sum_{n=1}^{L_j}\mathbf{m}_{j,n}^{(\mathrm{dl},1)}(\mathbf{m}_{j,n}^{(\mathrm{dl},1)})^{\mathrm{H}} + \sum_{r=2}^{N}\sum_{n=1}^{\bar{L}_r}\mathbf{v}_{r,n}^{(\mathrm{dl})}(\mathbf{v}_{r,n}^{(\mathrm{dl})})^{\mathrm{H}}\Big)\mathbf{H}_{1,k}^{\mathrm{H}} + \sum_{r=2}^{N}\sum_{j\in\mathcal{U}_r}\sum_{n=1}^{L_j}\tilde{\mathbf{H}}_{j,k}\mathbf{m}_{j,n}^{(\mathrm{ul},1)}(\tilde{\mathbf{H}}_{j,k}\mathbf{m}_{j,n}^{(\mathrm{ul},1)})^{\mathrm{H}} + \mathcal{N}_0\mathbf{I} \tag{6}$$

An intriguing relationship can be obtained between WQM and WSRM formulations by considering a special case of l_q-norm in the objective (assuming large queues at each node and q=1) [21], [36]. Moreover, both WSRM and WQM problems are known to be NP-hard even for the single antenna case [43]–[45]. However, computationally efficient solutions can be found by iterative alternating optimization (AO), similarly to [21], [36], [41]. First, by re-writing the rate terms using the corresponding MSE terms and introducing auxiliary MSE constraints as in [41] to (11), we can construct an approximated optimization problem as

$$\begin{aligned}\min_{\mathcal{M},\mathcal{W},\mathcal{T}} \sum_{k\in\mathcal{U}_1}\Big(&\alpha_k^{(\mathrm{dl})}(Q_k^{(\mathrm{dl})}-\sum_{l=1}^{L_k}J_0t_{k,l}^{(\mathrm{dl},1)})^q+\alpha_k^{(\mathrm{ul})}(Q_k^{(\mathrm{ul})}\\ &-\sum_{l=1}^{L_k}J_0t_{k,l}^{(\mathrm{ul},2)})^q\Big)+\sum_{i=2}^{N}\sum_{k\in\mathcal{U}_i}\Big(\alpha_k^{(\mathrm{ul})}(Q_k^{(\mathrm{ul})}-\sum_{l=1}^{L_k}J_0t_{k,l}^{(\mathrm{ul},1)})^q\\ &+\alpha_k^{(\mathrm{dl})}(Q_k^{(\mathrm{dl})}-\sum_{l=1}^{\bar{L}_i}a_k^{(\mathrm{dl})}J_0t_{i,l}^{(\mathrm{dl})})^q\\ &+\alpha_k^{(\mathrm{dl})}(\bar{Q}_k^{(\mathrm{dl})}+\sum_{l=1}^{\bar{L}_i}a_k^{(\mathrm{dl})}J_0t_{i,l}^{(\mathrm{dl})}-\sum_{l=1}^{L_k}J_0t_{k,l}^{(\mathrm{dl},2)})^q\\ &+\alpha_k^{(\mathrm{ul})}(\bar{Q}_k^{(\mathrm{ul})}+\sum_{l=1}^{L_k}J_0t_{k,l}^{(\mathrm{ul},1)}-\sum_{l=1}^{\bar{L}_i}a_k^{(\mathrm{ul})}J_0t_{i,l}^{(\mathrm{ul})})^q\Big), \qquad (12a)\end{aligned}$$

$$\text{s. t. } \epsilon_{k,l}^{(a,s)} \le \beta^{-t_{k,l}^{(a,s)}} \quad \forall(k,l), a \in \{\mathrm{dl},\mathrm{ul}\}, s\in\{1,2\}, \qquad (12b)$$

$$\epsilon_{i,l}^{(a)} \le \beta^{-t_{i,l}^{(a)}} \quad \forall i\in\mathbb{B}_{\mathrm{R}}\&\forall l, a\in\{\mathrm{dl},\mathrm{ul}\}, \qquad (12c)$$

$$(11b), (11c), (11d), (11e),$$

where $\mathcal{T}$ represents the set of the newly introduced auxiliary variables $t_{k,l}^{(a,s)}(\forall a,s,k,l)$, $t_{i,l}^{(a)}(\forall a,i,l)$. Also, $J_0=\log_2(\beta)$ and β is a predefined constant to adjust the approximation function such that $\beta>0$ [41]. By introducing these MSE constraints, the objective becomes a convex function of auxiliary variables $t_{k,l}^{(a,s)}$, $t_{i,l}^{(a)}$. However, MSE constraints in (12b) and (12c) are still non-convex, and that non-convexity is handled applying successive convex approximation (SCA) method, iteratively by using first-order Taylor series approximation [41]. For example, (12b) can be approximated as,

$$\beta^{-t_{k,l}^{(a,s)}} = -J_1t_{k,l}^{(a,s)}+J_2, \qquad (13)$$

where $J_1=\beta^{-\bar{t}_{k,l}^{(a,s)}}\log(\beta)$, $J_2=\beta^{-\bar{t}_{k,l}^{(a,s)}}+\bar{t}_{k,l}^{(a,s)}J_1$ and $\bar{t}_{k,l}^{(a,s)}$ is the point of approximation. For (12c), same approximation is applied as in (13). Then, by substituting approximated expressions in (13) to (12b) and (12c), the optimization problem in (12) can be efficiently solved using the KKT optimality conditions with the iterative AO method [36].

A. ALTERNATING OPTIMIZATION METHOD

Here, we present the iterative AO method using the KKT optimality conditions as follows; We begin by fixing the transmit precoders and solving for the receive beamformers and other variables (auxiliary and dual). First, we calculate the MMSE receivers using (7) and (36), then corresponding MSE values are obtained from (5) and (34). By using the complementary slackness of (12b) and (12c), we can update auxiliary variables $t_{k,l}^{(a,s)}$, $t_{i,l}^{(a)}$ as

$$t_{k,l}^{(a,s)} = \bar{t}_{k,l}^{(a,s)} + \frac{1}{\log(\beta)}\Big(1-\epsilon_{k,l}^{(a,s)}\beta^{\bar{t}_{k,l}^{(a,s)}}\Big), \qquad (14)$$

where $\bar{t}_{k,l}^{(a,s)}$ denotes $t_{k,l}^{(a,s)}$ from the previous iteration. This corresponds to a sub-gradient update of dual variable $t_{k,l}^{(a,s)}$ with step size $1/\log(\beta)$. Hence for the faster convergence, we can experiment with the step size as in [41]. Next, dual variables $\omega_{k,l}^{(a,s)}$, $\omega_{i,l}^{(a)}$ corresponding to (12b) and (12c) are obtained as

$$\omega_{k,l}^{(a,s)} = (1-\rho)\bar{\omega}_{k,l}^{(a,s)} + \rho\frac{qJ_0}{J_1}\Upsilon, \qquad (15)$$

where $\bar{\omega}_{k,l}^{(a,s)}$ denotes fixed $\omega_{k,l}^{(a,s)}$ from the previous iteration. Here, $\rho\in(0,1)$ controls the rate of convergence and is used to prevent over-allocation. For Rx1, Υ is given by

$$\Upsilon = \alpha_k^{(\mathrm{dl})}[(Q_k^{(\mathrm{dl})}-\sum_{l=1}^{L_k}J_0t_{k,l}^{(\mathrm{dl},1)})^{q-1}]^+, \qquad (16)$$

where $[x]^+\triangleq\max\{x,0\}$. For Rx2-Rx6, expressions for Υ is given in Appendix A.

Next, we fix the MMSE receivers and solve for the transmit precoders. The transmit precoders can be derived from the first-order optimality conditions of (12). Hence, transmit precoders for Tx1 transmitter type can be obtained as

$$\mathbf{m}_{k,l}^{(\mathrm{dl},1)} = \Big(\Phi_1^{(\mathrm{dl},1)}+\nu_1^{(\mathrm{dl},1)}\mathbf{I}\Big)^{-1}\omega_{k,l}^{(\mathrm{dl},1)}\mathbf{H}_{1,k}^{\mathrm{H}}\mathbf{u}_{k,l}^{(\mathrm{dl},1)}, \qquad (17)$$

where $\Phi_1^{(\mathrm{dl},1)}$ is the weighted transmit co-variance matrix and expression for $\Phi_1^{(\mathrm{dl},1)}$ is obtained as in (18) bottom of the next page. Also, $\nu_1^{(\mathrm{dl},1)}$, is the dual variable corresponding to power constraint in (11c). Hence, the transmit beamformers can efficiently solved from (17) by bisection search over the dual variables to satisfy the power constraint. For Tx2-Tx6, transmit precoder expressions are provided in Appendix A. Finally, we repeat above precoder/decoder optimization until the convergence of the objective function.

B. MULTIPLEXING BACKHAUL DATA

In the proposed beamformer design, we consider that backhaul carries multiple UE data at the same time either in UL or DL direction. Therefore, we define multiplexing factors $a_k^{(a)}$ to obtain individual user-specific rates via the backhaul link. Here, the multiplexing of user specific data over $\bar{L}_i$ backhaul streams assigned to RN i can be carried out using conventional approaches such as frequency-division-multiplexing (FDM) or time-division-multiplexing (TDM). In this subsection, we propose two approaches to calculate these multiplexing factors $a_k^{(a)}$; 1) KKT-based solution; 2) Heuristic method.

1) KKT-BASED SOLUTION

We can model these multiplexing factors $a_k^{(a)}$ as optimization variables in the original optimization problem in (12). In general, for any value of q in (12a), it is a tedious task to obtain a generalized closed-form solution for $a_k^{(a)}$ from KKT conditions as we have to find roots of a polynomial equation. However, for the specific case with $q = 2$, we can obtain optimized $a_k^{(a)}$ values by iteratively evaluating their corresponding KKT conditions (assuming fixed receive beamformers and auxiliary variables from the previous section). Note that $q > 2$ cases are left for future work. To this end, we introduce the following additional boundary constraints to the original optimization problem (12).

$$\sum_{k=1}^{|\mathcal{U}_i|} a_k^{(a)} = 1 \quad \forall i, \tag{19a}$$

$$a_k^{(a)} \geq 0 \quad \forall k. \tag{19b}$$

Then, by differentiating the modified Lagrangian (with $q = 2$) w.r.t to $a_k^{(a)}$ and applying the complementary slackness to the boundary constraints (19), we can obtain the following closed-form solution

$$a_k^{(a)} = [Z_k^{(a)} - v_i^{(a)}]^+, \tag{20}$$

where $v_i^{(a)}$ is the scaled dual variable corresponding to equality constraint (19a), and $Z_k^{(a)}$ is given by

$$Z_k^{(\mathrm{dl})} = (Q_k^{(\mathrm{dl})} - \bar{Q}_k^{(\mathrm{dl})} + \sum_{l=1}^{L_k} J_0 t_{k,l}^{(\mathrm{dl},2)})/2 \sum_{l=1}^{\bar{L}_i} J_0 t_{i,l}^{(\mathrm{dl})}. \tag{21a}$$

$$Z_k^{(\mathrm{ul})} = (\bar{Q}_k^{(\mathrm{ul})} + \sum_{l=1}^{L_k} J_0 t_{k,l}^{(\mathrm{ul},1)})/ \sum_{l=1}^{\bar{L}_i} J_0 t_{i,l}^{(\mathrm{ul})}. \tag{21b}$$

Here, $v_i^{(a)}, a_k^{(a)}$ are obtained by using a water-filling type algorithm such that $\sum_{k=1}^{|\mathcal{U}_i|}[Z_k^{(a)} - v_i^{(a)}]^+ = 1$. From the above solution, it is obvious that more backhaul resources are allocated to UEs with larger $Z_k^{(a)}$ values while no data is delivered to users with $Z_k^{(a)} - v_i^{(a)} < 0$. In each iteration $Z_k^{(a)}$ values change due to the iterative evaluation of the auxiliary variables. Thus, $a_k^{(a)}$ must be re-evaluated in each iteration until convergence.

2) HEURISTIC METHOD

In this method, we assign multiplexing factors $a_k^{(a)}$ based on the queue state of the UL and DL traffic and consider those as fixed values in the optimization problem (12). The proposed heuristic method is essential when we are unable to find optimization solution to $a_k^{(a)}$ (cases that $q \geq 3$) or when we need a simple practical solution.

Algorithm 1 Iterative Beamformer Design

1: Initializing feasible transmit beamformers $\mathbf{m}_{k,l}^{(a,s)}, \mathbf{v}_{i,l}^{(a)}$.
2: Calculate multiplexing factors $a_k^{(a)}$ for each UE using (22) (Heuristic method).
3: **repeat**
4: Estimate MMSE receivers $\mathbf{u}_{k,l}^{(a,s)}, \mathbf{w}_{i,l}^{(a)}$ by using (7) and (36).
5: Calculate MSE values $\epsilon_{k,l}^{(a,s)}, \epsilon_{i,l}^{(a)}$ from (5) and (34).
6: Calculate auxiliary variables $t_{k,l}^{(a,s)}, t_{i,l}^{(a)}$ from (14).
7: Calculate multiplexing factors $a_k^{(a)}$ for each UE from (20) (KKT based method).
8: Calculate dual variables $\omega_{k,l}^{(a,s)}, \omega_{i,l}^{(a)}$ using (15), (16) and (37).
9: Estimate transmit precoders $\mathbf{m}_{k,l}^{(a,s)}, \mathbf{v}_{i,l}^{(a)}$ from (17) and (38).
10: **until** convergence.

For the heuristic assignment of $a_k^{(a)}$, we make an assumption that the generated traffic in the system is delivered to the destination within two timeslots (no backlogged packets in the relay nodes). In such a case, we may assume that $\bar{Q}_k^{(a)} = 0$, $\sum_{l=1}^{L_k} J_0 t_{k,l}^{(\mathrm{dl},2)} = Q_k^{(\mathrm{dl})}$, $\sum_{l=1}^{L_k} J_0 t_{k,l}^{(\mathrm{ul},1)} = Q_k^{(\mathrm{ul})}$ and $\sum_{l=1}^{\bar{L}_i} J_0 t_{i,l}^{(a)} = \sum_{k=1}^{|\mathcal{U}_i|} Q_k^{(a)}$. Then, by substituting these values to (21)–(20) and applying boundary conditions, we can obtain $a_k^{(a)}$ simply as

$$a_k^{(a)} = \frac{Q_k^{(a)}}{\sum_{j=1}^{|\mathcal{U}_i|} Q_j^{(a)}}, \quad i \in \mathbb{B}_{\mathrm{R}}. \tag{22}$$

Finally, the complete iterative beamformer design with the proposed backhaul multiplexing schemes is summarized in Algorithm 1.

C. USER ASSIGNMENT

In this subsection, we propose a novel centralized approach to assign UEs into a particular BS or RN. Typically, UEs are assigned to their respective serving nodes based on the strongest received signal strength indicator (RSSI) value. However, that approach is not always a viable option for the IAB system, due to the asymmetric DL and UL data transmission and the spatial degree of freedom limitations for the BS-RN backhaul links. For example, two nearby UEs may be assigned to two different serving BS/RNs based on their RSSI values. Then, both UEs may suffer from significant UL-to-DL interference due to the different (UL and DL) transmission modes at BS, and RNs. To avoid this, we aim to assign nearby users into the same serving node. Moreover, RNs are often deployed in such a way that the BS-RN channel

$$\Phi_1^{(\mathrm{dl},1)} = \sum_{k\in\mathcal{U}_1}\sum_{l=1}^{L_j} \omega_{k,l}^{(\mathrm{dl},1)} \mathbf{H}_{1,k}^{\mathrm{H}} \mathbf{u}_{k,l}^{(\mathrm{dl},1)} (\mathbf{H}_{1,k}^{\mathrm{H}} \mathbf{u}_{k,l}^{(\mathrm{dl},1)})^{\mathrm{H}} + \sum_{i=2}^{N} \hat{\mathbf{H}}_{1,i}^{\mathrm{H}} (\sum_{l=1}^{\bar{L}_i} \omega_{i,l}^{(\mathrm{dl})} \mathbf{w}_{i,l}^{(\mathrm{dl})} (\mathbf{w}_{i,l}^{(\mathrm{dl})})^{\mathrm{H}} + \sum_{k\in\mathcal{U}_i}\sum_{l=1}^{L_j} \omega_{k,l}^{(\mathrm{ul},1)} \mathbf{u}_{k,l}^{(\mathrm{ul},1)} (\mathbf{u}_{k,l}^{(\mathrm{ul},1)})^{\mathrm{H}}) \hat{\mathbf{H}}_{1,i}. \tag{18}$$

has a line of sight (LOS) path. Hence, the fading channels between BS-RNs experience Rician fading statistics due to the dominant LOS component. With the LOS deployment, we may be able to have a reliable wireless backhaul between BS and RNs. However, at the same time, the number of parallel spatial streams available for the backhaul link is limited. The limited backhaul capacity may constitute a bottleneck for UEs served by RNs, as their incoming/outgoing traffic is relayed through the wireless in-band backhaul links. Therefore, such practical constraints unique to IAB systems are also considered in the proposed user assignment algorithm.

In the proposed user assignment approach, the BS collects the following information,

- Exact RSSI values between BS-UE and RN-UE links.
- Number of antennas and maximum transmit powers at each terminal.
- The multiplexing order of the BS-RN channels.
- Neighbouring UE information from each UEs based on the measured RSSI values between UE-UE links.

Initially, we calculate individual utility value $g_{i,k}$ for assigning an UE k to a particular BS or RN i. The cost value $g_{i,k}$ is expressed as

$$g_{i,k} = \log_2(1 + \frac{P_i^{(\mathrm{dl})} S_{i,k}}{M_i \mathcal{N}_0}), \tag{23}$$

where $S_{i,k}$ is the path gain between BS/RN i and UE k. The cost value $g_{i,k}$ represents a coarse prediction for the DL rate of UE k if served by BS/RN i. Next, the rank of the BS-RN channel for each backhaul link i is defined as

$$D_i = \mathrm{rank}(\hat{\mathbf{H}}_{1,i}) \qquad i \in \mathbb{B}_{\mathrm{R}}. \tag{24}$$

Also, the nearby UE set $\mathcal{Y}_k$ for each UE k potentially constituting high cross-link interference is given as

$$\mathcal{Y}_k = \{j \mid S_{j,k} > S_{\mathrm{th}} \quad \text{for } j = 1, \ldots, K\}, \tag{25}$$

where $S_{j,k}$ is the path gain between UE j and k, and S_{th} is a design parameter controlling the size $|\mathcal{Y}_k|$.

Each element $c_{i,k} \in \{0, 1\}$ in UE allocation matrix $\mathbf{C} \in \mathbb{B}^{N \times K}$ matrix represents assignment value of the UE k into BS/RN i, where $c_{i,k} = 1$ if the kth UE assigned into ith BS/RN, otherwise $c_{i,k} = 0$. Finally, the user assignment problem for IAB system can be formulated as

$$\max_{\mathbf{C}, A_i} \quad \sum_{i=1}^{N}\sum_{k=1}^{K} c_{i,k} g_{i,k} - \sum_{i=2}^{N} \zeta_i A_i \tag{26a}$$

$$\text{s. t. } A_i - (\sum_{k=1}^{K} c_{i,k} - D_i) \geq 0 \qquad i \in \mathbb{B}_{\mathrm{R}}, \tag{26b}$$

$$A_i \geq 0 \quad i \in \mathbb{B}_{\mathrm{R}}, \tag{26c}$$

$$\sum_{i=1}^{N} c_{i,k} = 1 \quad \forall k, \tag{26d}$$

$$c_{i,k} = \{0, 1\} \quad \forall i, k, \tag{26e}$$

$$c_{i,k} - c_{i,x} = 0 \quad \forall k, x \in \mathcal{Y}_k. \tag{26f}$$

where A_i denotes the number of UEs exceeding the spatial multiplexing capabilities of BS-RN link i and $\zeta_i > 0$ is a penalty value limiting the allocation of UEs to a specific RN much beyond the rank of the corresponding BS-RN channel. In the objective, we aim to find an optimal $c_{i,k} \in \{0, 1\}$ allocation to maximize the sum utility while penalizing the over-allocation of users into the RNs. Inequality constraints (26b) and (26c) make sure that the over-allocation penalty is always non-negative. The equality constraint (26d) guarantees that each UE is allocated into one serving BS/RN. The equality constraint (26f) aims to avoid large cross-link interference by forcing nearby users into the same BS/RN. Different approaches to solve the proposed user assignment problem are discussed below.

1) DIRECT LP SOLUTION

The user assignment problem in (26) is a combinatorial integer linear programming (ILP) problem [46]. The computational complexity of ILP increases exponentially with the number of BSs/RNs and UEs. However, we can find an approximated solution with greatly reduced complexity by relaxing the binary variable $c_{i,k}$ as a continuous variable $0 \leq c_{i,k} \leq 1$ and solving it as an LP problem. However, it is crucial to define nearby users set $\mathcal{Y}_k$ with properly planned interference threshold S_{th} to avoid assigning fractional $c_{i,k}$ values.

2) SCA BASED LP SOLUTION

As stated before, there is a chance to get fractional valued assignment matrix $\mathbf{C}$ from the direct LP solution due to an inadequate parameter setting or unfavorable user distribution. Hence, here we present a complementary method for the user assignment, which is still less complex than the ILP method but more scrupulous than the direct LP solution. In addition to relaxing the binary variables as continuous variables as in the direct LP solution, we introduce the following well-known sparsity inducing penalty function to the objective to enforce a binary solution [42]

$$f(\mathbf{C}) = \sum_{i=1}^{B}\sum_{k=1}^{K} \log(c_{i,k} + \delta), \tag{27}$$

where δ is a small positive constant used to limit the dynamic range of the log function. Moreover, to adapt the objective to the SCA framework, we linearize the penalty function by using first-order Taylor series approximation as [42]

$$f(\mathbf{C}^{(n+1)}) = f(\mathbf{C}^{(n)}) + \sum_{i=1}^{B}\sum_{k=1}^{K} \frac{c_{i,k} - c_{i,k}^{(n)}}{c_{i,k}^{(n)} + \delta}. \tag{28}$$

Now, with the linearized penalty (28) appended to the objective, the optimization problem in (26) can be solved as an iterative LP.

IV. PRACTICAL IMPLEMENTATION

In the previous section, we have proposed an iterative precoder/decoder design with the WQM objective for the IAB

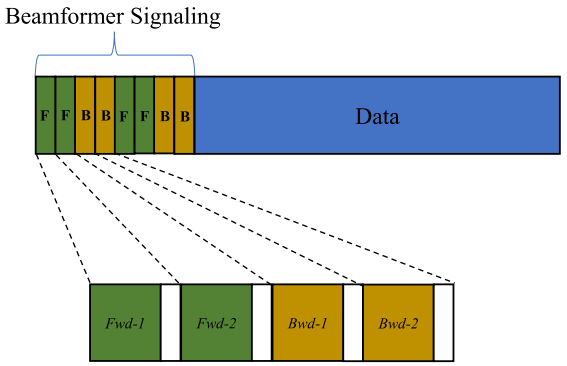

FIGURE 2. TDD frame structure.

system for a given user assignment. In principle, the proposed design summarized in Algorithm 1 can be implemented either in a centralized or decentralized manner. A specific challenge for the centralized implementation is the CSI acquisition of the cross-link interference channels, e.g., among mutually interfering user terminals. Explicit feedback of the UE-to-UE and RN-to-UE channels to the BS would be required to enable optimal beamformer design, which would make the centralized implementation infeasible in practice. On the other hand, the proposed coordinated node specific beamformer design can be implemented in a decentralized manner by employing bi-directional F-B training via spatially precoded OTA pilot signaling [22]–[24]. Here, our primary focus is on the detailed analysis of the decentralized implementation of the beamformer design in both ideal and non-ideal conditions.

A. TRAINING AND SIGNALING

The 5G 3GPP NR standard allows a large degree of flexibility to define application-specific frame structures. Specifically, due to the minislot concept introduced in NR, greatly expedited OTA information exchange is possible in both direction as already shown in our previous work [21].

For the decentralized design, we use specific TDD frame structure as shown in Fig. 2 [21]. The TDD frame is divided into two portions; 1) beamformer signaling; 2) data transmission. In the beamformer signaling phase, we employ precoded pilot sequences to exchange initial/intermediate beamformers and user-specific weights between coordinated nodes in both forward and backward directions iteratively. There, each node estimates their precoder/decoder based on the received forward/backward training sequences and the estimated precoder/decoder as the precoder for the next iteration forward/backward training. The forward and backward phases refer to the directions where the pilot training is aligned with or opposed to the data transmission, respectively. In the data transmission phase, the transmit precoders and receive decoders acquired after the last bi-directional training iteration are used for transmitting and receiving the data symbols.

There are two different beamformer estimation strategies, which can be used with bi-directional OTA signaling to obtain the transmit/receive beamformers; 1) direct beamformer estimation (DE), and 2) stream specific estimation (SSE). In the DE method, received precoded pilot training matrix is directly applied to estimate the required beamformer. On the other hand, in the SSE, each stream specific pilot sequence is decoded separately. Then, the estimated stream specific equivalent channels are used to construct the beamformers. Both schemes perform equally well in ideal conditions, such as employing orthogonal pilot sequences at each node with high SNR for estimation. However, the orthogonal pilot allocation is not typically possible for practical dense network deployments, especially with decentralized resource scheduling. Since the DE approach has shown good resilience to non-ideal conditions [21], [47], in this study, we focus on the DE method only.

TABLE 1. Pilot precoders and local feedbacks used during OTA bi-directional training.

Label	Tx nodes	OTA pilot precoders	Local feedbacks
Fwd-1	BS	$\mathbf{m}_{k,l}^{(\mathrm{dl},1)}, \mathbf{v}_{i,l}^{(\mathrm{dl})}$	$t_{i,l}^{(\mathrm{ul})}, t_{k,l}^{(\mathrm{dl},2)}$
	UEs served by RNs	$\mathbf{m}_{k,l}^{(\mathrm{ul},1)}$	NA
Fwd-2	UEs served by BS	$\mathbf{m}_{k,l}^{(\mathrm{ul},2)}$	NA
	RNs	$\mathbf{m}_{k,l}^{(\mathrm{dl},2)}, \mathbf{v}_{i,l}^{(\mathrm{ul})}$	$t_{i,l}^{(\mathrm{dl})}, t_{k,l}^{(\mathrm{ul},1)}$
Bwd-1	UEs served by BS	$\sqrt{\omega_{k,l}^{(\mathrm{dl},1)}}\mathbf{u}_{k,l}^{(\mathrm{dl},1)}$	$\omega_{k,l}^{(\mathrm{dl},1)}$
	RNs	$\sqrt{\omega_{i,l}^{(\mathrm{dl})}}\mathbf{w}_{i,l}^{(\mathrm{dl})}, \sqrt{\omega_{k,l}^{(\mathrm{ul},1)}}\mathbf{u}_{k,l}^{(\mathrm{ul},1)}$	$\omega_{i,l}^{(\mathrm{dl})}, \omega_{k,l}^{(\mathrm{ul},1)}$
Bwd-2	BS	$\sqrt{\omega_{i,l}^{(\mathrm{ul})}}\mathbf{w}_{i,l}^{(\mathrm{ul})}, \sqrt{\omega_{k,l}^{(\mathrm{dl},2)}}\mathbf{u}_{k,l}^{(\mathrm{dl},2)}$	$\omega_{i,l}^{(\mathrm{ul})}, \omega_{k,l}^{(\mathrm{dl},2)}$
	UEs served by RNs	$\sqrt{\omega_{k,l}^{(\mathrm{ul},2)}}\mathbf{u}_{k,l}^{(\mathrm{ul},2)}$	$\omega_{k,l}^{(\mathrm{ul},2)}$

B. DECENTRALIZED BEAMFORMER ESTIMATION

For the DE method, pilot precoders used for OTA bi-directional training and local scalar feedbacks are summarized in Table 1. In addition to the aforementioned OTA signaling, control feedback channels are used to explicitly exchange limited scalar-valued parameters related to initial queue states and the auxiliary variables of the local nodes (local nodes are referred to as immediate parent-child BS-RN, BS-UE and RN-UE pairs, and UE-UE pairs are not considered as local nodes). Details of the beamformer design steps at the transmit and receive nodes using OTA training and additional local feedback channels with minimal signaling are presented below.

1) RECEIVE BEAMFORMER AND WEIGHT ESTIMATION

The received precoded pilots information and explicit scalar valued local feedback information during *Fwd-1* and *Fwd-2* are used to estimate the receive beamformers, MSE values, user-specific weights, and auxiliary variables corresponding to the first and second timeslots, respectively.

Let $\mathbf{b}_{k,l}^{(a,s)} \in \mathbb{C}^S$ and $\mathbf{b}_{i,l}^{(s)} \in \mathbb{C}^S$ denote the pilot training sequences for l^{th} data stream corresponding to UE (UL or DL) k and RN i, respectively. Here, S is the length of the pilot sequence. In the forward training, the pilots are precoded with the transmit precoders $\mathbf{m}_{k,l}^{(a,s)}$ and $\mathbf{v}_{i,l}^{(a)}$. Then, the received

precoded pilot training matrix at DL UE $k \in \mathcal{U}_1$ during *Fwd-1* is given by

$$\mathbf{T}_k^{(\mathrm{dl},1)} = \mathbf{H}_{1,k}\Big(\sum_{j\in\mathcal{U}_1}\sum_{n=1}^{L_j}\mathbf{m}_{j,n}^{(\mathrm{dl},1)}\mathbf{b}_{j,n}^{(\mathrm{dl},1)} + \sum_{i=2}^{N}\sum_{n=1}^{\bar{L}_i}\mathbf{v}_{i,n}^{(\mathrm{dl})}\mathbf{b}_{i,n}^{(\mathrm{dl})}\Big) + \sum_{i=2}^{N}\sum_{j\in\mathcal{U}_i}\sum_{n=1}^{L_j}\tilde{\mathbf{H}}_{j,k}\mathbf{m}_{j,n}^{(\mathrm{ul},1)}\mathbf{b}_{j,n}^{(\mathrm{ul},1)} + \mathbf{N}_k, \quad (29)$$

where $\mathbf{N}_k \in \mathbb{C}^{N_k\times S}$ is the estimation noise matrix for all pilot symbols. Then, by using the received composite channel information $\mathbf{T}_k^{(\mathrm{dl},1)}$ and own pilot training sequence $\mathbf{b}_{k,l}^{(\mathrm{dl},1)}$ we can directly estimate the MMSE receivers as

$$\mathbf{u}_{k,l}^{(\mathrm{dl},1)} = \left(\mathbf{T}_k^{(\mathrm{dl},1)}\mathbf{T}_k^{(\mathrm{dl},1)^{\mathrm{H}}} + \mathcal{N}_0\mathbf{I}\right)^{-1}\mathbf{T}_k^{(\mathrm{dl},1)}\mathbf{b}_{k,l}^{(\mathrm{dl},1)^{\mathrm{H}}}. \quad (30)$$

Note that, the estimated MMSE receiver and the exact expression in (7) become identical, when training sequences are orthogonal, and SNR is high [21] (estimation noise vanishes). Next, the corresponding MSE can be estimated as

$$\epsilon_{k,l}^{(\mathrm{dl},1)} = 1 - \mathbf{u}_{k,l}^{(\mathrm{dl},1)^{\mathrm{H}}}\mathbf{T}_k^{(\mathrm{dl},1)}\mathbf{b}_{k,l}^{(\mathrm{dl},1)^{\mathrm{H}}}. \quad (31)$$

Similarly, for Rx2-Rx6, the received precoded matrices $\mathbf{T}_k^{(a,s)}\ \forall\ a,s,k$ and local stream specific pilot sequences $\mathbf{b}_{k,l}^{(a,s)}\ \forall\ a,s,k,l$ are used to estimate the corresponding MMSE receiver and MSE similarly to (30) and (31). Then, we can calculate node specific auxiliary variables $t_{k,l}^{(a,s)}$ as in (14), by using the estimated MSE values. Finally, user-specific weights $\omega_{k,l}^{(a,s)}$ are estimated using (15) and, (17) or (38). However, to do that, in addition to the OTA precoded information, we need explicit information on initial queues and auxiliary variables $(t_{k,l}^{(a,s)}, t_{i,l}^{(a)})$ from the local nodes. We assume this to be information exchange to happen over separate control feedback channels established among the local nodes. However, note that some of the feedback information can be outdated due to the inherent latency in the decentralized estimation.

2) TRANSMIT PRECODER ESTIMATION

The received precoded pilot information and local feedback information during *Bwd-1* and *Bwd-2* are used to estimate the transmit beamformers corresponding to the first and second timeslots, respectively.

During the backward training, the pilots are precoded with the weighted receivers $\sqrt{\omega_{k,l}^{(a,s)}}\mathbf{u}_{k,l}^{(a,s)}$ and $\sqrt{\omega_{i,l}^{(a)}}\mathbf{w}_{i,l}^{(a)}$. Then, the received precoded pilot training matrix at the BS during *Bwd-1* is given by

$$\mathbf{R}_1^{(\mathrm{dl},1)} = \sum_{i=2}^{N}\hat{\mathbf{H}}_{1,i}^{\mathrm{H}}\Big(\sum_{j\in\mathcal{U}_i}\sum_{n=1}^{L_j}\sqrt{\omega_{j,n}^{(\mathrm{ul},1)}}\mathbf{u}_{j,n}^{(\mathrm{ul},1)}\mathbf{b}_{j,n}^{(\mathrm{ul},1)} + \sum_{n=1}^{\bar{L}_i}\sqrt{\omega_{i,n}^{(\mathrm{dl})}}\mathbf{w}_{i,n}^{(\mathrm{dl})}\mathbf{b}_{i,n}^{(\mathrm{dl})}\Big) + \sum_{j\in\mathcal{U}_1}\sum_{n=1}^{L_j}\mathbf{H}_{1,j}^{\mathrm{H}}\sqrt{\omega_{j,n}^{(\mathrm{dl},1)}}\mathbf{u}_{j,n}^{(\mathrm{dl},1)}\mathbf{b}_{j,n}^{(\mathrm{dl},1)} + \mathbf{N}_1, \quad (32)$$

where $\mathbf{N}_1 \in \mathbb{C}^{M_1\times S}$ is the estimation noise matrix for all pilot symbols. Note that the forward and backward sequences are assumed to be the same, for any particular user. With the knowledge of the received training matrices, feedback information on local user-specific weights $(\omega_{k,l}^{(a,s)}, \omega_{i,l}^{(a)})$, and training sequences assigned to each locally served user, each transmit node can locally estimate their corresponding transmit beamformers. For example, transmit precoder for UE $k \in \mathcal{U}_1$ can be obtained in a closed-form expression as

$$\mathbf{m}_{k,l}^{(\mathrm{dl},1)} = \left(\mathbf{R}_1^{(\mathrm{dl},1)}\mathbf{R}_1^{(\mathrm{dl},1)^{\mathrm{H}}} + \mathbf{I}\nu_1^{(\mathrm{dl},1)}\right)^{-1}\sqrt{\omega_{k,l}^{(\mathrm{dl},1)}}\mathbf{R}_1^{(\mathrm{dl},1)}\mathbf{b}_{k,l}^{(\mathrm{dl},1)^{\mathrm{H}}}, \quad (33)$$

where the optimal $\nu_1^{(\mathrm{dl},1)}$ is found by bisection search to satisfy the power constraints (11c). Similarly, for Tx2-Tx6, the received precoded training matrices $\mathbf{R}_k^{(a,s)}, \mathbf{R}_i^{(a,s)}$, local stream specific pilot sequences $\mathbf{b}_{k,l}^{(a,s)}, \mathbf{b}_{i,l}^{(a)}$ and user-specific weights $\omega_{k,l}^{(a,s)}, \omega_{i,l}^{(a)}$ received over the feedback channels are used to estimate the transmit precoders. This transmit and receiver precoder estimation is carried out iteratively as in the previous case. Finally, we can summarize the proposed decentralized beamformer design as in Algorithm 2.

C. COMPLEXITY STUDY

In this subsection, we study the computational complexity of the proposed decentralized beamformer design. Since the complexity is linearly proportional to the number of OTA signaling rounds, we consider a single iteration only. The complexity at each node during the beamformer estimation is composed of the following.

- At the BS, both transmit and receive beamformers are estimated. For the transmit beamformer, the dominant operation is the matrix inversion in (33). Also, there is a dual variable that is found by bisection search to satisfy the power constraint. Hence, the complexity is $\mathcal{O}(M_1^3\Delta(K_1L_k + \sum_{i=2}^{N}\bar{L}_i))$, where Δ is the number bisection iterations required to satisfy the power constraint. Moreover, for receiver estimation, the dominant operation is the matrix product operation within the inverse matrix in (30). Hence the complexity is $\mathcal{O}(M_1^2S)$.
- At the UEs, the transmitter estimation complexity is $\mathcal{O}(N_k^3\Delta L_k)$ and the receiver estimation complexity is $\mathcal{O}(N_k^2S)$.
- Similarly, At RNs, the transmitter estimation complexity is $\mathcal{O}(M_i^3\Delta(K_iL_k + \bar{L}_i))$ and the receiver estimation complexity is $\mathcal{O}(M_i^2S)$.

According to the complexity study, the BS should have a higher computational capability compared to UEs and RNs. Note that due to the decentralized and parallel computation of the precoders at BS and RNs, the computational complexity per one OTA signaling cycle considerably is in the same

Algorithm 2 Decentralized Beamformer Design Assist With Bi-Directional Training and Local Feedbacks

1: Initialize transmit precoders $(\mathbf{m}_{k,l}^{(a,s)}, \mathbf{v}_{i,l}^{(a)})$.
2: Calculate multiplexing factors $a_k^{(a)}$ for each UE using (22) (Heuristic method).
3: Exchange UL/DL queues $(Q_k^{(a)}, \bar{Q}_k^{(a)})$, prioritizing weights $(\alpha_k^{(a)})$, initial auxiliary variables $(t_{i,l}^{(a)}, t_{k,l}^{(a,s)})$ and multiplexing factors $(a_k^{(a)})$ between local nodes via feedback channels.
4: **repeat**
5: *Fwd-1*: BS and UEs served by RNs send OTA pilots precoded with transmit beamformers $\mathbf{m}_{k,l}^{(a,1)}, \mathbf{v}_{i,l}^{(\mathrm{dl})}$. Exchange auxiliary variables $t_{i,l}^{(\mathrm{ul})}, t_{k,l}^{(\mathrm{dl},2)}$ (initial or previously calculated during *Fwd-2*) to local nodes via feedback.
6: RNs and UEs served by BS estimate MMSE receivers $\mathbf{u}_{k,l}^{(a,1)}, \mathbf{w}_{i,l}^{(\mathrm{dl})}$ from (30), and calculate auxiliary variables $t_{k,l}^{(a,1)}, t_{i,l}^{(\mathrm{dl})}$ from (14) and user-specific weights $\omega_{k,l}^{(a,1)}, \omega_{i,l}^{(\mathrm{dl})}$ from (15).
7: *Fwd-2*: RNs and UEs served by BS send OTA pilots precoded with transmit beamformers $\mathbf{m}_{k,l}^{(a,2)}, \mathbf{v}_{i,l}^{(\mathrm{ul})}$. Exchange auxiliary variables $t_{i,l}^{(\mathrm{dl})}, t_{k,l}^{(\mathrm{ul},1)}$ (calculated during *Fwd-1*) to local nodes via feedback.
8: BS and UEs served by RNs estimate MMSE receivers $\mathbf{u}_{k,l}^{(a,2)}, \mathbf{w}_{i,l}^{(\mathrm{ul})}$ from (30) and calculate auxiliary variables $t_{k,l}^{(a,2)}, t_{i,l}^{(\mathrm{ul})}$ from (14) and user-specific weights $\omega_{k,l}^{(a,2)}, \omega_{i,l}^{(\mathrm{ul})}$ from (15).
9: *Bwd-1*: RNs and UEs served by BS send OTA pilots precoded with weighted MMSE receivers $\sqrt{\omega_{k,l}^{(a,1)}}\mathbf{u}_{k,l}^{(a,1)}, \sqrt{\omega_{i,l}^{(\mathrm{dl})}}\mathbf{w}_{k,l}^{(\mathrm{dl})}$. Exchange user-specific weights $\omega_{k,l}^{(a,1)}, \omega_{i,l}^{(\mathrm{dl})}$ to local nodes via feedback.
10: BS and UEs served by RNs estimate transmit precoders $\mathbf{m}_{k,l}^{(a,1)}, \mathbf{v}_{i,l}^{(\mathrm{dl})}$ from (33).
11: *Bwd-2*: The BS and UEs served by RNs send OTA pilots precoded with intermediate weighted MMSE receivers $\sqrt{\omega_{k,l}^{(a,2)}}\mathbf{u}_{k,l}^{(a,2)}, \sqrt{\omega_{i,l}^{(\mathrm{ul})}}\mathbf{w}_{k,l}^{(\mathrm{ul})}$. Exchange user-specific weights $\omega_{k,l}^{(a,2)}, \omega_{i,l}^{(\mathrm{ul})}$ to local nodes via feedback.
12: RNs and UEs served by BS estimate transmit precoders $\mathbf{m}_{k,l}^{(a,2)}, \mathbf{v}_{i,l}^{(\mathrm{ul})}$ from (33).
13: **until** convergence.

range as any other multiuser MIMO MMSE-type single-hop beamformer designs [34], [36], [41].

V. NUMERICAL EXAMPLES

In the simulation model, we consider a symmetric IAB model with one BS and four RNs, with 200m distance between BS and each RN. The number of BS, RN and UE antennas is $M_1 = 20$, $M_i = 8$ and $N_k = 2$, respectively. The power constraint for BS is normalized to $P_1 = 10$, and power

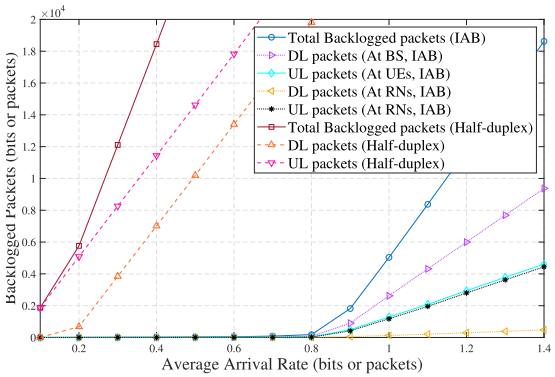

FIGURE 3. Comparison of IAB model with conventional HD relaying system after 1000 traffic arrivals for $K_i = 4\ \forall i$.

constraints at RNs and UEs are $P_i = P_1/4$ and $p_k = P_1/20$ (to have similar UL and DL power levels in both timeslots), respectively. Noise power $(\mathcal{N}_0)$ is obtained assuming the cell edge (100m from BS) SNR for BS transmission to be 10 dB (SNR $= S_{1,k}P_1^{(\mathrm{dl})}/\mathcal{N}_0$). Also, the path loss exponent is 3.67. We consider uncorrelated i.i.d fading for BS-UE and RN-UE channels. The BS-RN channels in Figs. 3 and 4 are modelled as uncorrelated i.i.d while correlated Rician fading is assumed for the rest of the figures. Also, for Figs. 7 to 9, we consider $D_i = 2\ \forall i \in \mathbb{B}_{\mathrm{R}}$ and path gain threshold for nearby user set $S_{\mathrm{th}} = 15^{-3.67}$. We consider Poisson arrival process to generate the traffic in the network, where $\lambda_k^{(\mathrm{a})}(\tau) \sim$ **Pois**$(A_k^{(\mathrm{a})})$ is the generated traffic for DL/UL UE k in time instance τ. Here, $A_k^{(\mathrm{a})} = \mathbb{E}_\tau\{\lambda_k^{(\mathrm{a})}\}$ are the average number of packet arrivals in bits for the corresponding UL/DL UEs. Then, the total number of queued packets in each UL/DL queue at $(\tau+1)^{th}$ time instant is given by $Q_k^{(a)}(\tau+1) = \left[Q_k^{(a)}(\tau) - R_k^{(a)}(\tau)\right]^+ + \lambda_k^{(a)}(\tau)$, where $R_k^{(a)}$ is the transmission rate to/from UE k. Also, the user priority weights (α_k) are assumed to be 1. Except for the Fig. 5, rest of the figures are limited to 10 beamformer iterations per scheduling interval (TDD frame) due to practical limitations in OTA beamformer training process.

It should be noted that the choice of the symmetric placement of RNs was fairly arbitrary and mainly based on the ability to reproduce the results easily. However, the proposed beamformer design is independent of the simulation setup and works for any asymmetric deployment as well. Indeed, the user-specific rates and backhaul rates depend on the link distance given a limited power budget at each node. Hence, from the queue minimization perspective, given the same traffic arrival rate per user, the weakest backhaul links would dominate the accumulated total backlog packets in the network. In practice, arrival rate should be adjusted for users served by more distant RNs. The optimal placement of RNs is given practical constraints imposed by the proposed IAB setup is an interesting idea for future extension of the current work.

The average total backlogged packets after 1000 traffic arrivals (which is equivalent to 2000 timeslots) in the system

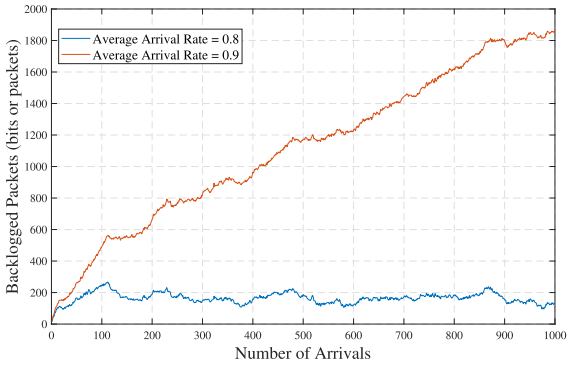

FIGURE 4. Total backlogged packets in the IAB system with the number of traffic arrivals for $K_i = 4\ \forall i$.

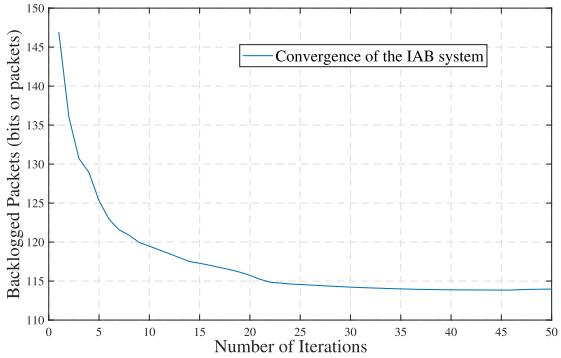

FIGURE 5. Convergence behaviour of the proposed iterative beamformer design for IAB system with $K_i = 4\ \forall i$.

queues versus average traffic arrival rate is shown in Fig. 3, where UEs are randomly placed within 50m from the serving BS/RN. As the reference case, we consider a conventional HD relaying system, which takes two timeslots for each UL and DL data transmission. In the HD system, we assume 50% of the time, it is in DL mode, and the rest of the time, it is in UL mode. We can observe that, despite the increased cross-link interference, flexible TDD based IAB system always performs much better in comparison to the HD relaying system in all traffic arrival rates. The IAB system becomes unstable after the arrival rate reaches 0.9 (after that queues grow linearly with the arrival rate), while the HD case gets saturated with much lower arrival rates. Also, we can observe that RN queues are in general less congested than the queues at UEs and at BS. Hence, the RNs can potentially have smaller buffer sizes without deteriorating the system performance. Fig. 4 illustrates the total backlogged packets in the IAB system with the number of packet arrivals. For the arrival rate 0.8, the system is in a stable region where the total number of backlogged traffic fluctuate around 200 bits. However, when the average arrival rate is at 0.9, the IAB system becomes unstable and queues grow without limit. Thus, for the considered simulation model, the proposed WQM based beamformer design is able to optimally utilize network resources up to arrival rate 0.8 while satisfying all the UE demands.

It should be noted that the beamformers are designed to follow the dynamic traffic arrival process, where each node is assigned resources based on their instantaneous queue states both in UL and DL. Therefore, in such dynamic environment, the beamformers never really converge but they keep adapting to instantaneous traffic load while minimizing the total (weighted) queues in the network over time. However, for a static snapshot of the dynamic process, the convergence behaviour of the proposed beamformer design can be studied. Fig. 5 illustrates the convergence of the algorithm at one particular time instance (with 0.8 arrival rate) averaged over a large number of channel realizations. The results demonstrate that even though it takes about 20 iterations to reach a point where the objective is not improved anymore, most of the improvement occurs during thew first few iterations. This a desired feature for an algorithm which aims at following a dynamic traffic arrival process.

The performance of the IAB system for different antenna configurations are represented in Fig. 6. As expected, the stable region increases with the number of antennas both at BS and RNs. Again, in all the cases, IAB system shows superior performance in comparison to the reference case with HD relays. The performance of the proposed user assignment algorithm with $K = 20$ after 1000 random user drops is presented in Fig. 7. Those results are generated using the direct LP solution that we have proposed to the optimization problem in (26) (Note that the SCA based LP solution provides quite similar results for the chosen parameter set). The left figure shows average number of UEs assigned to BS and each RN. There, on average, half of the UEs are assigned to BS while other half is assigned to rest of the RNs. Due to the symmetrical placement of the RNs around the BS, on average, UEs are equally assigned to RNs. Also, when a UE drops in the middle of the BS and a RN, that particular UE is most likely assigned to BS. The right figure illustrates CDF of the assignment values ($c_{i,k}$). We can observe that 80% of the time $c_{i,k}$ value takes 0, and for the rest of the time, it takes 1. We hardly observe any fractional values are assigned to $c_{i,k}$. Hence, the proposed design assigns only 0s and 1s to the assignment matrix as desired.

The performance of the IAB system after 1000 traffic arrivals with the proposed user assignment algorithm is shown in Fig.8. The proposed user assignment algorithm is labelled as 'UA'. In the reference case, labelled as C-UE, UEs are assigned to BS or RN based on the strongest RSSI value. We can observe that with the proposed user assignment method, the performance of the system is improved compared to the traditional RSSI based user assignment for all $K = \{15, 20, 25\}$. Increasing the total number of UEs K, the stable region of the IAB system is decreased due to the limited power budget and degrees of freedom.

In Fig.9, the performance of the IAB system is shown after 1000 traffic arrivals when employing non-orthogonal random pilots for OTA training with the decentralized

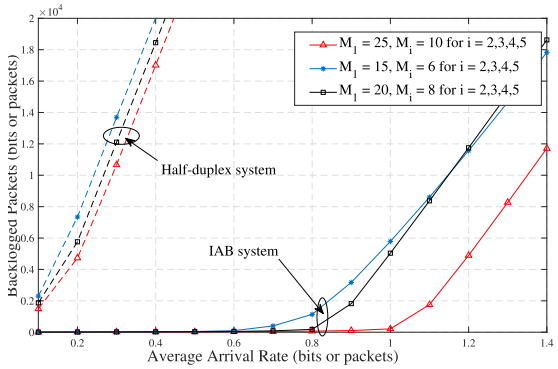

FIGURE 6. IAB system performance for different antenna configurations at BS and RNs with $K_i = 4\ \forall i$.

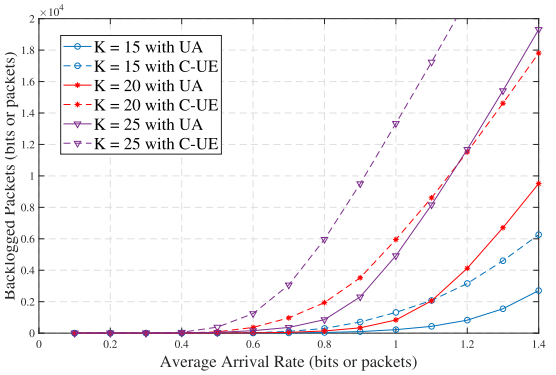

FIGURE 8. Average total backlogged packets of the system with the user assignment algorithm.

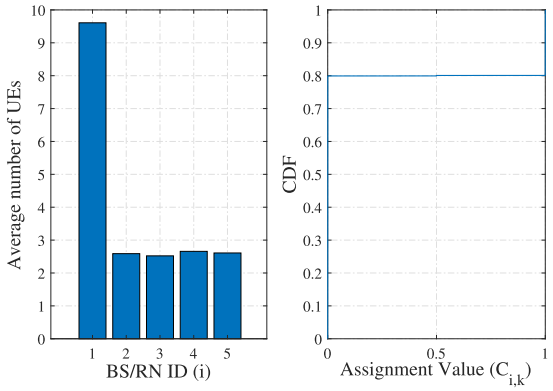

FIGURE 7. Performance of the user assignment algorithm with $K = 20$; Left figure: Average number of UEs assigned into each BS/RN; Right figure: CDF of the assignment values $c_{i,k}$.

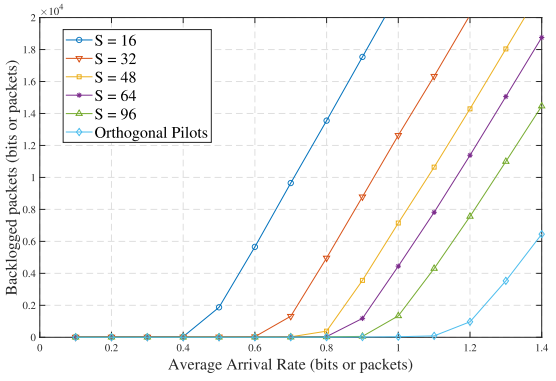

FIGURE 9. IAB system performance of the decentralized implementation by using OTA bi-directional training with non-orthogonal pilot sequences for $K = 20$.

beamformer implementation. Also, a 10 dB pilot boost is used in the simulations. For the considered model, ideally 48 orthogonal pilot sequences (2 for each user and 2 for each BS-RN link) would be required to carry out the OTA bi-directional training without any pilot contamination (assuming the same pilot is used for forward and backward training). Therefore, we can observe that the decentralized random pilot allocation is greatly deteriorated if shorter sequence lengths ($S = 16, 32$) are used due to the high level of pilot contamination. However, the decentralized pilot assignment starts to perform reasonably well with $S = 48$, and with $S = 96$, it can withstand about 80% of the traffic load provided by the centralized (orthogonal) pilot allocation.

VI. CONCLUSION

In this paper, a flexible TDD based IAB system was investigated with complex interference conditions due to simultaneous UL/DL traffic, in-band access, and backhaul traffic. Decentralized coordinated multiantenna beamforming techniques were applied to mitigate the interference with the WQM objective. Queue dynamics at each node over two timeslots were jointly considered in the beamformer design. The original NP-hard optimization problem was solved to get a computationally efficient solution by

$$\mathbf{M}_i^{(\mathrm{ul},1)} = \hat{\mathbf{H}}_{1,i}\Big(\sum_{j\in\mathcal{U}_1}\sum_{n=1}^{L_j}\mathbf{m}_{j,n}^{(\mathrm{dl},1)}(\mathbf{m}_{j,n}^{(\mathrm{dl},1)})^{\mathrm{H}} + \sum_{r=2}^{N}\sum_{n=1}^{\bar{L}_r}\mathbf{v}_{r,n}^{(\mathrm{dl})}(\mathbf{v}_{r,n}^{(\mathrm{dl})})^{\mathrm{H}}\Big)\hat{\mathbf{H}}_{1,i}^{\mathrm{H}} + \sum_{r=2}^{N}\sum_{j\in\mathcal{U}_r}\sum_{n=1}^{L_j}\mathbf{H}_{i,j}^{\mathrm{H}}\mathbf{m}_{j,n}^{(\mathrm{ul},1)}(\mathbf{H}_{i,j}^{\mathrm{H}}\mathbf{m}_{j,n}^{(\mathrm{ul},1)})^{\mathrm{H}} + \mathcal{N}_0\mathbf{I}.$$

$$\mathbf{M}_1^{(\mathrm{ul},2)} = \sum_{r=2}^{N}\hat{\mathbf{H}}_{1,r}^{\mathrm{H}}\Big(\sum_{n=1}^{\bar{L}_r}\mathbf{v}_{r,n}^{(\mathrm{ul})}(\mathbf{v}_{r,n}^{(\mathrm{ul})})^{\mathrm{H}} + \sum_{j\in\mathcal{U}_r}\sum_{n=1}^{L_j}\mathbf{m}_{j,n}^{(\mathrm{dl},2)}(\mathbf{m}_{j,n}^{(\mathrm{dl},2)})^{\mathrm{H}}\Big)\hat{\mathbf{H}}_{1,r} + \sum_{j\in\mathcal{U}_1}\sum_{n=1}^{L_j}\mathbf{H}_{1,j}^{\mathrm{H}}\mathbf{m}_{j,n}^{(\mathrm{ul},2)}(\mathbf{H}_{1,j}^{\mathrm{H}}\mathbf{m}_{j,n}^{(\mathrm{ul},2)})^{\mathrm{H}} + \mathcal{N}_0\mathbf{I}.$$

$$\mathbf{M}_k^{(\mathrm{dl},2)} = \sum_{r=1}^{N}\mathbf{H}_{r,k}\Big(\sum_{n=1}^{\bar{L}_r}\mathbf{v}_{r,n}^{(\mathrm{ul})}(\mathbf{v}_{r,n}^{(\mathrm{ul})})^{\mathrm{H}} + \sum_{j\in\mathcal{U}_r}\sum_{n=1}^{L_j}\mathbf{m}_{j,n}^{(\mathrm{dl},2)}(\mathbf{m}_{j,n}^{(\mathrm{dl},2)})^{\mathrm{H}}\Big)\mathbf{H}_{r,k}^{\mathrm{H}} + \sum_{j\in\mathcal{U}_1}\sum_{n=1}^{L_j}\tilde{\mathbf{H}}_{j,k}^{\mathrm{H}}\mathbf{m}_{j,n}^{(\mathrm{ul},2)}(\tilde{\mathbf{H}}_{j,k}^{\mathrm{H}}\mathbf{m}_{j,n}^{(\mathrm{ul},2)})^{\mathrm{H}} + \mathcal{N}_0\mathbf{I}. \quad (35)$$

using iterative AO method. Backhaul rate multiplexing was introduced to the original optimization problem and corresponding rate multiplexing terms were solved either directly via KKT-based algorithm or simple heuristic method. Novel centralized user assignment algorithm was proposed by solving a combinatorial optimization problem to support IAB functionality and WQM objective. Distributed implementation of the beamformer design was carried out by using the OTA bi-directional signaling framework and robust LS based direct beamformer estimation. In numerical examples, flexible TDD based IAB system with the proposed beamformer design user assignment scheme showed superior performance in comparison to the conventional HD relaying system. Furthermore, IAB-nodes can potentially be equipped with smaller buffer sizes without compromising the system performance. Finally, DE based coordinated beamformer design was proposed using precoded pilots in OTA bi-directional signaling and explicit scalar feedbacks. It was shown to perform reasonably well by alleviating the pilot contamination even with relatively short non-orthogonal pilot sequence lengths.

APPENDIX A

A. AMSE, RECEIVED SIGNAL COVARIANCE AND MMSE RECEIVER EXPRESSIONS FOR Rx2-Rx6

MSE expressions for receiver type Rx2-Rx6 is given by

$$\epsilon_{k,l}^{(s,a)}/\epsilon_{i,l}^{(a)} = \begin{cases} 1-2\Re(\mathbf{u}_{k,l}^{(\mathrm{ul},1)^{\mathrm{H}}}\mathbf{H}_{i,k}^{\mathrm{H}}\mathbf{m}_{k,l}^{(\mathrm{ul},1)}) + \mathbf{u}_{k,l}^{(\mathrm{ul},1)^{\mathrm{H}}}\mathbf{M}_{i}^{(\mathrm{ul},1)}\mathbf{u}_{k,l}^{(\mathrm{ul},1)}, & \text{Rx2} \\ 1-2\Re(\mathbf{w}_{i,l}^{(\mathrm{dl})^{\mathrm{H}}}\hat{\mathbf{H}}_{1,i}\mathbf{v}_{i,l}^{(\mathrm{dl})}) + \mathbf{w}_{i,l}^{(\mathrm{dl})^{\mathrm{H}}}\mathbf{M}_{i}^{(\mathrm{ul},1)}\mathbf{w}_{i,l}^{(\mathrm{dl})}, & \text{Rx3} \\ 1-2\Re(\mathbf{u}_{k,l}^{(\mathrm{ul},2)^{\mathrm{H}}}\mathbf{H}_{1,k}^{\mathrm{H}}\mathbf{m}_{k,l}^{(\mathrm{ul},2)}) + \mathbf{u}_{k,l}^{(\mathrm{ul},2)^{\mathrm{H}}}\mathbf{M}_{1}^{(\mathrm{ul},2)}\mathbf{u}_{k,l}^{(\mathrm{ul},2)}, & \text{Rx4} \\ 1-2\Re(\mathbf{u}_{k,l}^{(\mathrm{dl},2)^{\mathrm{H}}}\mathbf{H}_{i,k}\mathbf{m}_{k,l}^{(\mathrm{dl},2)}) + \mathbf{u}_{k,l}^{(\mathrm{dl},2)^{\mathrm{H}}}\mathbf{M}_{k}^{(\mathrm{dl},2)}\mathbf{u}_{k,l}^{(\mathrm{dl},2)}, & \text{Rx5} \\ 1-2\Re(\mathbf{w}_{i,l}^{(\mathrm{ul})^{\mathrm{H}}}\hat{\mathbf{H}}_{1,i}^{\mathrm{H}}\mathbf{v}_{i,l}^{(\mathrm{ul})}) + \mathbf{w}_{k,l}^{(\mathrm{ul})^{\mathrm{H}}}\mathbf{M}_{1}^{(\mathrm{ul},2)}\mathbf{w}_{i,l}^{(\mathrm{ul})}, & \text{Rx6} \end{cases} \tag{34}$$

where $\mathbf{M}_{i}^{(\mathrm{ul},1)} = \mathbb{E}[\mathbf{x}_{i}^{(\mathrm{ul},1)}(\mathbf{x}_{i}^{(\mathrm{ul},1)})^{\mathrm{H}}]$, $\mathbf{M}_{1}^{(\mathrm{ul},2)} = \mathbb{E}[\mathbf{x}_{1}^{(\mathrm{ul},2)}(\mathbf{x}_{1}^{(\mathrm{ul},2)})^{\mathrm{H}}]$, and $\mathbf{M}_{k}^{(\mathrm{dl},2)} = \mathbb{E}[\mathbf{x}_{k}^{(\mathrm{dl},2)}(\mathbf{x}_{k}^{(\mathrm{dl},2)})^{\mathrm{H}}]$ are the received signal covariance matrices at each node, which are given in (35) bottom of the previous page. Then, the corresponding MMSE receivers are given by

$$\tilde{\mathbf{u}}_{k,l}^{(a,s)}/\tilde{\mathbf{w}}_{i,l}^{(a)} = \begin{cases} (\mathbf{M}_{i}^{(\mathrm{ul},1)})^{-1}\mathbf{H}_{i,k}^{\mathrm{H}}\mathbf{m}_{k,l}^{(\mathrm{ul},1)}, & \text{Rx2} \\ (\mathbf{M}_{i}^{(\mathrm{ul},1)})^{-1}\hat{\mathbf{H}}_{1,i}\mathbf{v}_{i,l}^{(\mathrm{dl})}, & \text{Rx3} \\ (\mathbf{M}_{1}^{(\mathrm{ul},2)})^{-1}\mathbf{H}_{1,k}^{\mathrm{H}}\mathbf{m}_{k,l}^{(\mathrm{ul},2)}, & \text{Rx4} \\ (\mathbf{M}_{k}^{(\mathrm{dl},2)})^{-1}\mathbf{H}_{i,k}\mathbf{m}_{k,l}^{(\mathrm{dl},2)}, & \text{Rx5} \\ (\mathbf{M}_{1}^{(\mathrm{ul},2)})^{-1}\hat{\mathbf{H}}_{1,i}^{\mathrm{H}}\mathbf{v}_{i,l}^{(\mathrm{ul})}. & \text{Rx6} \end{cases} \tag{36}$$

B. EXPRESSIONS FOR Υ

For Rx2-Rx6, Υ is given by

$$\Upsilon = \begin{cases} \alpha_{k}^{(\mathrm{ul})}[(Q_{k}^{(\mathrm{ul})} - \sum_{l=1}^{L_k} J_0 t_{k,l}^{(\mathrm{ul},1)})^{q-1} - (\bar{Q}_{k}^{(\mathrm{ul})} \\ + \sum_{l=1}^{L_k} J_0 t_{k,l}^{(\mathrm{ul},1)} - \sum_{l=1}^{\bar{L}_i} a_{k}^{(\mathrm{ul})} J_0 t_{i,l}^{(\mathrm{ul})})^{q-1}]^{+}, & \text{Rx2} \\ [\sum_{k\in\mathcal{U}_i} \alpha_{k}^{(\mathrm{dl})} a_{k}^{(\mathrm{dl})}((Q_{k}^{(\mathrm{dl})} \\ - \sum_{l=1}^{\bar{L}_i} a_{k}^{(\mathrm{dl})} J_0 t_{i,l}^{(\mathrm{dl})})^{q-1} \\ -(\bar{Q}_{k}^{(\mathrm{dl})} + \sum_{l=1}^{\bar{L}_i} a_{k}^{(\mathrm{dl})} J_0 t_{i,l}^{(\mathrm{dl})} \\ - \sum_{l=1}^{L_k} J_0 t_{k,l}^{(\mathrm{dl},2)})^{q-1})]^{+}, & \text{Rx3} \\ \alpha_{k}^{(\mathrm{ul})}[(Q_{k}^{(\mathrm{ul})} - \sum_{l=1}^{L_k} J_0 t_{k,l}^{(\mathrm{ul},2)})^{q-1}]^{+}, & \text{Rx4} \\ \alpha_{k}^{(\mathrm{dl})}[(\bar{Q}_{k}^{(\mathrm{dl})} + \sum_{l=1}^{\bar{L}_i} a_{k}^{(\mathrm{dl})} J_0 t_{i,l}^{(\mathrm{dl})} \\ - \sum_{l=1}^{L_k} J_0 t_{k,l}^{(\mathrm{dl},2)})^{q-1}]^{+}, & \text{Rx5} \\ [\sum_{k\in\mathcal{U}_i} \alpha_{k}^{(\mathrm{ul})} a_{k}^{(\mathrm{ul})}((\bar{Q}_{k}^{(\mathrm{ul})} + \sum_{l=1}^{L_k} J_0 t_{k,l}^{(\mathrm{ul},1)} \\ - \sum_{l=1}^{\bar{L}_i} a_{k}^{(\mathrm{ul})} J_0 t_{i,l}^{(\mathrm{ul})})^{q-1})]^{+}, & \text{Rx6} \end{cases} \tag{37}$$

C. TRANSMIT PRECODER EXPRESSIONS FOR Tx2-Tx6

Expressions for transmit precoders are given by

$$\mathbf{m}_{k,l}^{(a,s)}/\mathbf{v}_{i,l}^{(a)} = \begin{cases} \left(\Phi_{k}^{(\mathrm{ul},1)} + \nu_{k}^{(\mathrm{ul},1))}\mathbf{I}\right)^{-1}\omega_{k,l}^{(\mathrm{ul},1))}\mathbf{H}_{i,k}\mathbf{u}_{k,l}^{(\mathrm{ul},1)}, & \text{Tx2} \\ \left(\Phi_{1}^{(\mathrm{dl},1)} + \nu_{1}^{(\mathrm{dl},1)}\mathbf{I}\right)^{-1}\omega_{i,l}^{(\mathrm{dl})}\hat{\mathbf{H}}_{1,i}^{\mathrm{H}}\mathbf{w}_{i,l}^{(\mathrm{dl})}, & \text{Tx3} \\ \left(\Phi_{k}^{(\mathrm{ul},2)} + \nu_{k}^{(\mathrm{ul},2)}\mathbf{I}\right)^{-1}\omega_{k,l}^{(\mathrm{ul},2)}\mathbf{H}_{1,k}\mathbf{u}_{k,l}^{(\mathrm{ul},2)}, & \text{Tx4} \\ \left(\Phi_{i}^{(\mathrm{dl},2)} + \nu_{i}^{(\mathrm{dl},2)}\mathbf{I}\right)^{-1}\omega_{k,l}^{(\mathrm{dl},2)}\mathbf{H}_{i,k}^{\mathrm{H}}\mathbf{u}_{k,l}^{(\mathrm{dl},2)}, & \text{Tx5} \\ \left(\Phi_{i}^{(\mathrm{dl},2)} + \nu_{i}^{(\mathrm{dl},2)}\mathbf{I}\right)^{-1}\omega_{i,l}^{(\mathrm{ul})}\mathbf{H}_{1,i}\mathbf{w}_{k,l}^{(\mathrm{ul})}. & \text{Tx6} \end{cases} \tag{38}$$

$$\Phi_{k}^{(\mathrm{ul},1)} = \sum_{j\in\mathcal{U}_1}\sum_{l=1}^{L_j}\omega_{j,l}^{(\mathrm{dl},1)}\tilde{\mathbf{H}}_{j,k}^{\mathrm{H}}\mathbf{u}_{j,l}^{(\mathrm{dl},1)}(\tilde{\mathbf{H}}_{j,k}^{\mathrm{H}}\mathbf{u}_{j,l}^{(\mathrm{dl},1)})^{\mathrm{H}} + \sum_{i=2}^{N}\mathbf{H}_{i,k}(\sum_{l=1}^{\bar{L}_i}\omega_{i,l}^{(\mathrm{dl})}\mathbf{w}_{i,l}^{(\mathrm{dl})}(\mathbf{w}_{i,l}^{(\mathrm{dl})})^{\mathrm{H}} + \sum_{j\in\mathcal{U}_i}\sum_{l=1}^{L_j}\omega_{j,l}^{(\mathrm{ul},1)}\mathbf{u}_{j,l}^{(\mathrm{ul},1)}(\mathbf{u}_{j,l}^{(\mathrm{ul},1)})^{\mathrm{H}})\mathbf{H}_{i,k}^{\mathrm{H}}.$$

$$\Phi_{k}^{(\mathrm{ul},2)} = \sum_{i=2}^{N}\sum_{j\in\mathcal{U}_i}\sum_{n=1}^{L_j}\omega_{j,l}^{(\mathrm{dl},2)}\tilde{\mathbf{H}}_{j,k}^{\mathrm{H}}\mathbf{w}_{j,l}^{(\mathrm{dl},2)}(\tilde{\mathbf{H}}_{j,k}^{\mathrm{H}}\mathbf{w}_{j,l}^{(\mathrm{dl},2)})^{\mathrm{H}} + \mathbf{H}_{1,k}(\sum_{i=2}^{N}\sum_{l=1}^{\bar{L}_i}\omega_{i,l}^{(\mathrm{ul})}\mathbf{w}_{i,l}^{(\mathrm{ul})}(\mathbf{w}_{i,l}^{(\mathrm{ul})})^{\mathrm{H}} + \sum_{j\in\mathcal{U}_1}\sum_{l=1}^{L_j}\omega_{j,l}^{(\mathrm{ul},2)}\mathbf{u}_{j,l}^{(\mathrm{ul},2)}(\mathbf{u}_{j,l}^{(\mathrm{ul},2)})^{\mathrm{H}})\mathbf{H}_{1,k}^{\mathrm{H}}.$$

$$\Phi_{i}^{(\mathrm{dl},2)} = \sum_{r=2}^{N}\sum_{j\in\mathcal{U}_r}\sum_{n=1}^{L_j}\omega_{j,l}^{(\mathrm{dl},2)}\mathbf{H}_{i,j}^{\mathrm{H}}\mathbf{w}_{j,l}^{(\mathrm{dl},2)}(\mathbf{H}_{i,j}^{\mathrm{H}}\mathbf{w}_{j,l}^{(\mathrm{dl},2)})^{\mathrm{H}} + \mathbf{H}_{1,i}(\sum_{i=2}^{N}\sum_{l=1}^{\bar{L}_i}\omega_{i,l}^{(\mathrm{ul})}\mathbf{w}_{i,l}^{(\mathrm{ul})}(\mathbf{w}_{i,l}^{(\mathrm{ul})})^{\mathrm{H}} + \sum_{j\in\mathcal{U}_1}\sum_{l=1}^{L_j}\omega_{j,l}^{(\mathrm{ul},2)}\mathbf{u}_{j,l}^{(\mathrm{ul},2)}(\mathbf{u}_{j,l}^{(\mathrm{ul},2)})^{\mathrm{H}})\mathbf{H}_{1,i}^{\mathrm{H}}. \tag{39}$$

where $\Phi_k^{(\mathrm{ul},1)}$, $\Phi_k^{(\mathrm{ul},2)}$ and $\Phi_i^{(\mathrm{dl},2)}$ are the weighted transmit covariance matrices, which are given in (39) bottom of the previous page. Also, $\nu_k^{((\mathrm{ul},1)}$, $\nu_k^{(\mathrm{ul},2)}$ and $\nu_i^{(\mathrm{dl},2)}$ are the dual variables corresponding to the power constraints in (11b), (11d) and (11e), respectively.

ACKNOWLEDGMENT

This article was presented in part at the IEEE WCNC, Virtual Conference, 2020.

REFERENCES

[1] Cisco Systems. (Sep. 2017). *Cisco Visual Networking Index: Forecast and Methodology, 2016-2021*. [Online]. Available: https://www.cisco.com/c/en/us/solutions/collateral/service-provider/visual-networking-index-vni/complete-white-paper-c11-481360.pdf

[2] T. Nakamura, S. Nagata, A. Benjebbour, Y. Kishiyama, T. Hai, S. Xiaodong, Y. Ning, and L. Nan, "Trends in small cell enhancements in LTE advanced," *IEEE Commun. Mag.*, vol. 51, no. 2, pp. 98–105, Feb. 2013.

[3] W. Saad, M. Bennis, and M. Chen, "A vision of 6G wireless systems: Applications, trends, technologies, and open research problems," Feb. 2019, *arXiv:1902.10265*. [Online]. Available: http://arxiv.org/abs/1902.10265

[4] D. Hui and J. Axnas, "Joint routing and resource allocation for wireless self-backhaul in an indoor ultra-dense network," in *Proc. IEEE 24th Annu. Int. Symp. Pers., Indoor, Mobile Radio Commun. (PIMRC)*, Sep. 2013, pp. 3083–3088.

[5] R. Baldemair, T. Irnich, K. Balachandran, E. Dahlman, G. Mildh, Y. Selén, S. Parkvall, M. Meyer, and A. Osseiran, "Ultra-dense networks in millimeter-wave frequencies," *IEEE Commun. Mag.*, vol. 53, no. 1, pp. 202–208, Jan. 2015.

[6] *Study on Integrated Access and Backhaul*, document NR TR 38.874, 3GPP, 2018. [Online]. Available: http://www.3gpp.org

[7] *Study on Security Aspects of Integrated Access and Backhaul (IAB) for Next Radio (NR)*, document TR 33.824, 3GPP, 2019. [Online]. Available: http://www.3gpp.org

[8] J. N. Laneman, D. N. C. Tse, and G. W. Wornell, "Cooperative diversity in wireless networks: Efficient protocols and outage behavior," *IEEE Trans. Inf. Theory*, vol. 50, no. 12, pp. 3062–3080, Dec. 2004.

[9] G. Kramer, M. Gastpar, and P. Gupta, "Cooperative strategies and capacity theorems for relay networks," *IEEE Trans. Inf. Theory*, vol. 51, no. 9, pp. 3037–3063, Sep. 2005.

[10] P. Jayasinghe, L. K. S. Jayasinghe, M. Juntti, and M. Latva-Aho, "Performance analysis of optimal beamforming in fixed-gain AF MIMO relaying over asymmetric fading channels," *IEEE Trans. Commun.*, vol. 62, no. 4, pp. 1201–1217, Apr. 2014.

[11] U. Siddique, H. Tabassum, and E. Hossain, "Downlink spectrum allocation for in-band and out-band wireless backhauling of full-duplex small cells," *IEEE Trans. Commun.*, vol. 65, no. 8, pp. 3538–3554, Aug. 2017.

[12] H. Shen, W. Xu, S. Gong, Z. He, and C. Zhao, "Statistically robust beamforming optimization for multi-antenna full-duplex DF relaying," *IEEE Access*, vol. 7, pp. 175564–175575, 2019.

[13] Y. Cai, Y. Xu, Q. Shi, B. Champagne, and L. Hanzo, "Robust joint hybrid transceiver design for millimeter wave full-duplex MIMO relay systems," *IEEE Trans. Wireless Commun.*, vol. 18, no. 2, pp. 1199–1215, Feb. 2019.

[14] R. Gupta and S. Kalyanasundaram, "Resource allocation for self-backhauled networks with half-duplex small cells," in *Proc. IEEE Int. Conf. Commun. Workshops (ICC Workshops)*, May 2017, pp. 198–204.

[15] S. Hong, J. Brand, J. Choi, M. Jain, J. Mehlman, S. Katti, and P. Levis, "Applications of self-interference cancellation in 5G and beyond," *IEEE Commun. Mag.*, vol. 52, no. 2, pp. 114–121, Feb. 2014.

[16] B. Rankov and A. Wittneben, "Spectral efficient protocols for half-duplex fading relay channels," *IEEE J. Sel. Areas Commun.*, vol. 25, no. 2, pp. 379–389, Feb. 2007.

[17] S. S. Ikki and S. Aissa, "Performance analysis of two-way amplify-and-forward relaying in the presence of co-channel interferences," *IEEE Trans. Commun.*, vol. 60, no. 4, pp. 933–939, Apr. 2012.

[18] K. Jayasinghe, P. Jayasinghe, N. Rajatheva, and M. Latva-Aho, "Secure beamforming design for physical layer network coding based MIMO two-way relaying," *IEEE Commun. Lett.*, vol. 18, no. 7, pp. 1270–1273, Jul. 2014.

[19] *Study on New Radio Access Technology Physical Layer Aspects*, document TR 38.802, 3GPP, 2017. [Online]. Available: http://www.3gpp.org

[20] J. Kaleva, A. Tolli, G. Venkatraman, and M. Juntti, "Downlink precoder design for coordinated regenerative multi-user relaying," *IEEE Trans. Signal Process.*, vol. 61, no. 5, pp. 1215–1229, Mar. 2013.

[21] P. Jayasinghe, A. Tolli, J. Kaleva, and M. Latva-aho, "Bi-directional beamformer training for dynamic TDD networks," *IEEE Trans. Signal Process.*, vol. 66, no. 23, pp. 6252–6267, Dec. 2018.

[22] P. Komulainen, A. Tolli, and M. Juntti, "Effective CSI signaling and decentralized beam coordination in TDD multi-cell MIMO systems," *IEEE Trans. Signal Process.*, vol. 61, no. 9, pp. 2204–2218, May 2013.

[23] C. Shi, R. A. Berry, and M. L. Honig, "Bi-directional training for adaptive beamforming and power control in interference networks," *IEEE Trans. Signal Process.*, vol. 62, no. 3, pp. 607–618, Feb. 2014.

[24] A. Tolli, H. Ghauch, J. Kaleva, P. Komulainen, M. Bengtsson, M. Skoglund, M. Honig, E. Lahetkangas, E. Tiirola, and K. Pajukoski, "Distributed coordinated transmission with forward-backward training for 5G radio access," *IEEE Commun. Mag.*, vol. 57, no. 1, pp. 58–64, Jan. 2019.

[25] E. G. Larsson, O. Edfors, F. Tufvesson, and T. L. Marzetta, "Massive MIMO for next generation wireless systems," *IEEE Commun. Mag.*, vol. 52, no. 2, pp. 186–195, Feb. 2014.

[26] R. Brandt and M. Bengtsson, "Distributed CSI acquisition and coordinated precoding for TDD multicell MIMO systems," *IEEE Trans. Veh. Technol.*, vol. 65, no. 5, pp. 2890–2906, May 2016.

[27] M. Heino, D. Korpi, T. Huusari, E. Antonio-Rodriguez, S. Venkatasubramanian, T. Riihonen, L. Anttila, C. Icheln, K. Haneda, R. Wichman, and M. Valkama, "Recent advances in antenna design and interference cancellation algorithms for in-band full duplex relays," *IEEE Commun. Mag.*, vol. 53, no. 5, pp. 91–101, May 2015.

[28] A. Sabharwal, P. Schniter, D. Guo, D. W. Bliss, S. Rangarajan, and R. Wichman, "In-band full-duplex wireless: Challenges and opportunities," *IEEE J. Sel. Areas Commun.*, vol. 32, no. 9, pp. 1637–1652, Sep. 2014.

[29] L. Sanguinetti, A. L. Moustakas, and M. Debbah, "Interference management in 5G reverse TDD HetNets with wireless backhaul: A large system analysis," *IEEE J. Sel. Areas Commun.*, vol. 33, no. 6, pp. 1187–1200, Jun. 2015.

[30] R. Louie, Y. Li, and B. Vucetic, "Practical physical layer network coding for two-way relay channels: Performance analysis and comparison," *IEEE Trans. Wireless Commun.*, vol. 9, no. 2, pp. 764–777, Feb. 2010.

[31] R. Zhang, Y.-C. Liang, C. C. Chai, and S. Cui, "Optimal beamforming for two-way multi-antenna relay channel with analogue network coding," *IEEE J. Sel. Areas Commun.*, vol. 27, no. 5, pp. 699–712, Jun. 2009.

[32] A. Y. Panah and P. Sartori, "System and method for two-way relaying with beamforming," U.S. Patent 10 256 873, Apr. 9, 2019.

[33] V. Havary-Nassab, S. Shahbazpanahi, and A. Grami, "Optimal distributed beamforming for two-way relay networks," *IEEE Trans. Signal Process.*, vol. 58, no. 3, pp. 1238–1250, Mar. 2010.

[34] S. S. Christensen, R. Agarwal, E. De Carvalho, and J. M. Cioffi, "Weighted sum-rate maximization using weighted MMSE for MIMO-BC beamforming design," *IEEE Trans. Wireless Commun.*, vol. 7, no. 12, pp. 4792–4799, Dec. 2008.

[35] Q. Shi, M. Razaviyayn, Z.-Q. Luo, and C. He, "An iteratively weighted MMSE approach to distributed sum-utility maximization for a MIMO interfering broadcast channel," *IEEE Trans. Signal Process.*, vol. 59, no. 9, pp. 4331–4340, Sep. 2011.

[36] G. Venkatraman, A. Tolli, M. Juntti, and L.-N. Tran, "Traffic aware resource allocation schemes for multi-cell MIMO-OFDM systems," *IEEE Trans. Signal Process.*, vol. 64, no. 11, pp. 2730–2745, Jun. 2016.

[37] R. R. Muller, L. Cottatellucci, and M. Vehkapera, "Blind pilot decontamination," *IEEE J. Sel. Topics Signal Process.*, vol. 8, no. 5, pp. 773–786, Oct. 2014.

[38] H. Yin, D. Gesbert, M. C. Filippou, and Y. Liu, "Decontaminating pilots in massive MIMO systems," in *Proc. IEEE Int. Conf. Commun. (ICC)*, vol. 2013, pp. 3170–3175.

[39] J. Jose, A. Ashikhmin, T. L. Marzetta, and S. Vishwanath, "Pilot contamination and precoding in multi-cell TDD systems," *IEEE Trans. Wireless Commun.*, vol. 10, no. 8, pp. 2640–2651, Aug. 2011.

[40] E. Bjornson, J. Hoydis, and L. Sanguinetti, "Pilot contamination is not a fundamental asymptotic limitation in massive MIMO," in *Proc. IEEE Int. Conf. Commun. (ICC)*, May 2017, pp. 1–6.

[41] J. Kaleva, A. Tolli, and M. Juntti, "Decentralized sum rate maximization with QoS constraints for interfering broadcast channel via successive convex approximation," *IEEE Trans. Signal Process.*, vol. 64, no. 11, pp. 2788–2802, Jun. 2016.
[42] G. Venkatraman, A. Tolli, M. Juntti, and L.-N. Tran, "Multigroup multicast beamformer design for MISO-OFDM with antenna selection," *IEEE Trans. Signal Process.*, vol. 65, no. 22, pp. 5832–5847, Nov. 2017.
[43] C. T. Ng and H. Huang, "Linear precoding in cooperative MIMO cellular networks with limited coordination clusters," *IEEE J. Sel. Areas Commun.*, vol. 28, no. 9, pp. 1446–1454, Dec. 2010.
[44] Z.-Q. Luo and S. Zhang, "Dynamic spectrum management: Complexity and duality," *IEEE J. Sel. Topics Signal Process.*, vol. 2, no. 1, pp. 57–73, Feb. 2008.
[45] S. Shi, M. Schubert, and H. Boche, "Downlink MMSE transceiver optimization for multiuser MIMO systems: Duality and sum-MSE minimization," *IEEE Trans. Signal Process.*, vol. 55, no. 11, pp. 5436–5446, Nov. 2007.
[46] S. Boyd and L. Vandenberghe, *Convex Optimization*. Cambridge, U.K.: Cambridge Univ. Press, 2004.
[47] J. Kaleva, A. Tolli, M. Juntti, R. A. Berry, and M. L. Honig, "Decentralized joint precoding with pilot-aided beamformer estimation," *IEEE Trans. Signal Process.*, vol. 66, no. 9, pp. 2330–2341, May 2018.

PRANEETH JAYASINGHE (Member, IEEE) received the B.Sc. (Eng.) degree in electronics and telecommunications engineering from the University of Moratuwa, Sri Lanka, in 2009, and the M.Sc. (Tech.) degree in wireless communication engineering from the University of Oulu, Oulu, Finland, in 2014, where he is currently pursuing the Ph.D. degree with the Department of Communication Engineering. His research interest includes resource allocation on flexible TDD based heterogeneous wireless networks.

ANTTI TÖLLI (Senior Member, IEEE) received the D.Sc. (Tech.) degree in electrical engineering from the University of Oulu, Oulu, Finland, in 2008. From 1998 to 2003, he worked with Nokia Networks as a Research Engineer and a Project Manager both in Finland and Spain. In May 2014, he was granted a five year (2014–2019) Academy Research Fellow post by the Academy of Finland. During the academic year 2015–2016, he visited at EURECOM, Sophia Antipolis, France, while from August 2018 till June 2019, he was visiting with the University of California, Santa Barbara, USA. He is currently an Associate Professor with the Center for Wireless Communications (CWC), University of Oulu. He has authored numerous articles in peer-reviewed international journals and conferences and several patents all in the area of signal processing and wireless communications. His research interests include radio resource management and transceiver design for broadband wireless communications with a special emphasis on distributed interference management in heterogeneous wireless networks. He is also serving as an Associate Editor for IEEE TRANSACTIONS ON SIGNAL PROCESSING.

JARKKO KALEVA (Member, IEEE) received the D.Sc. (Tech.) degree (Hons.) in communications engineering from the University of Oulu, Oulu, Finland, in 2018. In 2010, he joined the Center for Wireless Communications (CWC), University of Oulu. He is currently a Co-Founder of Solmu Technologies Oy, where he is also working as the Chief Software Architect. His research interests include nonlinear programming, dynamic systems, and deep learning.

MATTI LATVA-AHO (Senior Member, IEEE) received the M.Sc., Lic.Tech., and D.Tech. (Hons.) degrees in electrical engineering from the University of Oulu, Finland, in 1992, 1996, and 1998, respectively. From 1992 to 1993, he was a Research Engineer with Nokia Mobile Phones, Oulu, Finland, after which he joined the Center for Wireless Communications (CWC), University of Oulu. He was the Director of CWC from 1998 to 2006, and the Head of the Department for Communication Engineering until August 2014. He has been serving as the Academy of Finland Professor since 2017, and the Director for National 6G Flagship Programme since 2018. His research interests are related to mobile communication systems and currently his group focuses on 5G and beyond systems research. He has published close to 500 conference or journal articles in the field of wireless communications. He received Nokia Foundation Award in 2015 for his achievements in mobile communications research.